15

The search for supersymmetry at colliders

While the first clear hints of deviation from the SM may well come from any of a large variety of experiments, establishing precisely what the new physics is will be possible only by observations at energy scales close to, or beyond, the threshold for the new phenomena. Direct examination of the properties of any new states of matter associated with the new physics is probably the best way to study the new phenomena, if these degrees of freedom are kinematically accessible. If the new physics is supersymmetry, then the new states of matter will be the superpartners, and it is only by determining their quantum numbers and couplings that we can unambiguously establish that the new physics is actually supersymmetry. Of course, any new states of matter may be quite different from superpartners. For instance, if extra spatial dimensions exist which are accessible at the weak scale, the new degrees of freedom will be Kaluza–Klein excitations of SM particles. It is even possible that no new degrees of freedom are directly accessible, but that SM interactions acquire form factors that point to what the new physics might be. Our point here is that elucidation of new physics will only be possible at colliding beam facilities.

The purpose of this chapter is to examine what may be learned from a study of high energy collisions assuming that nature is supersymmetric at the weak scale. To start with, we review various searches for supersymmetry in previous collider and fixed target experiments. Up to now, no direct evidence for SUSY has been found. The negative searches have been interpreted as lower limits on sparticle masses, and as exclusion of regions of the parameter space of various specific models for MSSM sparticle masses. Next, we project the SUSY reach of the luminosity upgrade of the Fermilab Tevatron $p\bar{p}$ collider with $\sqrt{s} = 2$ TeV that has already begun operation, as well as of the CERN Large Hadron Collider (LHC), a 14 TeV $p\bar{p}$ collider scheduled to commence operation in 2007. We also discuss the capability of a high energy e^+e^- linear collider (LC) operating at $\sqrt{s} = 0.5$–1 TeV for SUSY studies; such a machine is being considered for construction in the not-too-distant future. In the latter part of the chapter we discuss how a determination of sparticle properties at

https://doi.org/10.1017/9781009289801.016 Published online by Cambridge University Press

the LHC and at a LC may be used to establish that the new physics is supersymmetry and, further, to zero in on the mechanism by which MSSM superpartners acquire SUSY breaking masses and couplings. Our discussion follows a "bottom-up" vision of a program for high energy physics over the next two decades that includes the following general steps:

- Establish the discovery of new physics.
- Figure out what the new physics is – here, we take it to be weak scale supersymmetry.
- From the experimentally determined values of sparticle masses and couplings, figure out the organizing principle(s) that lead to the observed supersymmetry breaking parameters.

Interpretation of negative results of searches for supersymmetric particles depends heavily on the assumptions made about the underlying supersymmetric model. Many sparticle search experiments try to be as model independent as possible, in which case limits can be placed on sparticle masses. But sometimes dependence on a model for a particular analysis is unavoidable. In these cases, null search results are often presented as limits on model parameter space in one or two-parameter space dimensions. Other model parameters can be scanned over, so that results apply for a wide range of model parameters. Alternatively, results can be presented for "typical" choices of other model parameters, such as $\tan\beta$. Finally, bounds can be presented as a function of the model parameter which gives the most conservative estimate of the reach into parameter space.

15.1 Early searches for supersymmetry

Experiments at the energy frontier have been searching for supersymmetry since the early 1980s when it was recognized that weak scale supersymmetry could protect the large hierarchy between the weak and GUT (or Planck) scales from large radiative corrections.

15.1.1 e^+e^- collisions

Searches for supersymmetry were performed in the early 1980s at the PEP e^+e^- collider at SLAC ($\sqrt{s} \simeq 29$ GeV) by the MAC and MARK 2 collaborations and at the PETRA e^+e^- collider at DESY ($\sqrt{s} \lesssim 47$ GeV) by the MARK J, CELLO, TASSO, and JADE collaborations. The center of mass energy was extended in the mid to late 1980s by the TOPAZ, VENUS, and AMY experiments at the Tristan e^+e^- collider operating at KEK at $\sqrt{s} \lesssim 60$ GeV.

https://doi.org/10.1017/9781009289801.016 Published online by Cambridge University Press

Typically, the searches focussed on signals from the lightest charged sparticles since these could be produced with relatively large cross sections. It was assumed that any sparticles which were produced would promptly decay to the LSP (which was assumed to be photino-like). The relevant processes searched for were:

$$e^+e^- \to \tilde{\ell}^+\tilde{\ell}^- \to \ell^+\ell^-\widetilde{Z}_1\widetilde{Z}_1, \tag{15.1a}$$

$$e^+e^- \to \tilde{q}\bar{\tilde{q}} \to q\bar{q}\widetilde{Z}_1\widetilde{Z}_1, \tag{15.1b}$$

and

$$e^+e^- \to \widetilde{W}_1\overline{\widetilde{W}}_1 \to f_i\bar{f}'_i\widetilde{Z}_1 + f_j\bar{f}'_j\widetilde{Z}_1, \tag{15.2}$$

where f and f' are the upper and lower members of a weak $SU(2)$ doublet, and the subscripts i and j denote the fermion type. Since the neutralino LSPs would escape undetected in the experimental apparatus, the experimental signature for slepton (squark) production was taken to be a pair of acolinear leptons (jets) balanced by missing energy and missing transverse momentum carried off by the LSPs. Chargino pair production can lead to missing energy events with multiple jets, jets and a charged lepton, or a charged lepton pair, depending on how the charginos decay. Within the SM, missing energy can only arise if neutrinos are produced in the reaction in addition to the charged leptons and/or jets. The SM cross section for events with hard jets and/or leptons together with large missing energy is very small, and the non-observation of an excess of signal events above expected background levels is interpreted as a lower limit on $m_{\tilde{\ell}}$, $m_{\tilde{q}}$, and $m_{\widetilde{W}_1}$. In addition, there are non-physics backgrounds from experimental mismeasurements that can fake missing energy events. These backgrounds depend on the energy resolution of the experimental apparatus, and also on other details such as uninstrumented regions of this detector, etc. and so are detector-dependent. By selecting events to lie in a kinematic region with large $E_{\mathrm{T}}^{\mathrm{miss}}$, these backgrounds can be greatly suppressed. The residual background is usually evaluated using event simulation programs discussed in the previous chapter, interfaced with programs to simulate the response of the experimental apparatus. Because the background rate is small, the non-observation of a signal translates into a lower limit only a little below the beam energy. Mass limits on selectrons (whose cross section is enhanced by t-channel $\widetilde{Z}_1$ exchange) and charginos (whose cross section has an s-wave threshold compared to the p-wave threshold for sfermion production) were somewhat stronger than the limits placed on the other sfermions.

Assuming that the $\widetilde{Z}_1$ ($\tilde{\nu}_e$) is very light and escapes detection, the MAC, ASP, and AMY collaborations were able to obtain lower limits on $m_{\tilde{e}}$ ($m_{\widetilde{W}_1}$) beyond the kinematic limit for selectron (chargino) pair production by searching for single

https://doi.org/10.1017/9781009289801.016 Published online by Cambridge University Press

photon events coming from

$$e^+e^- \to \widetilde{Z}_1\widetilde{Z}_1\gamma \quad \text{or} \quad \tilde{\nu}_e\bar{\tilde{\nu}}_e\gamma, \tag{15.3}$$

where the first of these takes place via selectron exchange and the second via chargino exchange. The SM background from $e^+e^- \to \nu\bar{\nu}\gamma$ production is very small. Non-observation of these single photon events has also been re-interpreted as excluding portions of the selectron–goldstino mass plane. This search is also relevant in models with a very light gravitino.

15.1.2 Searches at the CERN S$p\bar{p}$S collider

Shortly after the inauguration in 1982 of the CERN S$p\bar{p}$S collider at $\sqrt{s} = 546$ GeV and the discovery of the W and Z bosons, a variety of anomalous collider events were reported by the UA1 and UA2 collaborations: these included events containing one or more jets plus missing transverse energy at UA1 and, at UA2, events containing a hard electron plus jets plus $E_{\mathrm{T}}^{\mathrm{miss}}$. The UA1 events were exactly the sort of events expected from pair production of gluinos or squarks with $m \sim 40$–50 GeV, depending on which is the lighter: the produced sparticles were assumed to decay directly to the LSP either via $\tilde{g} \to q\bar{q}\widetilde{Z}_1$, or via $\tilde{q} \to q\widetilde{Z}_1$. The excitement was short-lived as it was soon realized that SM processes such as $q\bar{q} \to Z + g$ or $q\bar{q}' \to W + g$ followed by $Z \to \nu\bar{\nu}$ or $W \to \tau\nu_\tau$ could give rise to these jet(s) $+E_{\mathrm{T}}^{\mathrm{miss}}$ events at the observed rates.

Subsequently, the collider energy was raised to $\sqrt{s} = 630$ GeV and SM backgrounds to the $E_{\mathrm{T}}^{\mathrm{miss}}$ data sample were carefully estimated. UA1 was able to place limits of $m_{\tilde{g}} > 53$ GeV and $m_{\tilde{q}} > 45$ GeV, assuming degenerate squark masses and a neutralino with mass less than 20 GeV. Their results could not exclude gluinos with mass less than 4 GeV, leaving open a window for a light gluino. The UA2 experiment, ultimately taking more data than UA1, was able to raise the lower bounds to $m_{\tilde{q}} > 74$ GeV and $m_{\tilde{g}} > 79$ GeV, but the light gluino window still remained open.

15.1.3 A light gluino window?

Gluinos with lifetimes long compared to the hadronization time will bind with a gluon or with $q\bar{q}$ pairs to form neutral or charged R-parity odd hadrons before decaying to the LSP. The lightest of these R-odd hadrons is expected to be neutral, and is denoted by R^0. R-hadrons in the mass range 1.5–7.5 GeV can be produced by strong interactions via collisions of protons on nuclear targets. During the late 1970s, several fixed target experiments obtained upper limits on the cross sections of a neutral hadron decaying into a final state containing a charged hadron, excluding various ranges of $m_{\tilde{g}}$ depending on its lifetime.

https://doi.org/10.1017/9781009289801.016 Published online by Cambridge University Press

Gluinos were searched for but not found in neutrino beam dump experiments by looking for the re-interaction of the LSP produced via $\tilde{g} \to q\bar{q}\widetilde{Z}_1$ by the WA-66, E-613 and CHARM collaborations. These searches, which exclude portions of the $m_{\tilde{g}} - \tau_{\tilde{g}}$ plane, become ineffective for large squark masses (long gluino lifetimes) because the neutralino interaction cross section falls as $1/m_{\tilde{q}}^4$. Light gluinos were also searched for by the WA-75 collaboration in π meson beam dumps onto emulsions, again with a negative result.

Light gluinos were also searched for in $\Upsilon \to \eta_{\tilde{g}}\gamma$ decays by the CUSB experiment, where $\eta_{\tilde{g}}$ is the pseudoscalar $\tilde{g}\tilde{g}$ bound state. The non-observation of monoenergetic photons excludes $1.5 \leq m_{\tilde{g}} \leq 3$ GeV, independent of the gluino lifetime. The ARGUS experiment searched for gluinos via $\chi_b \to \tilde{g}\tilde{g}g$ decays, with one of the R-hadrons decaying away from the interaction point, and excluded the mass range 1–4.5 GeV for an appropriate lifetime range.

Despite these efforts, a window for light gluinos still remained, where the R^0 hadron was expected to have a mass of 1–3 GeV and a lifetime of 10^{-10}–10^{-5} s. The R^0 was expected to decay mainly via $R^0 \to \rho\widetilde{Z}_1 \to \pi^+\pi^-\widetilde{Z}_1$ and at smaller rates into the C-violating mode $R^0 \to \pi^0\widetilde{Z}_1$. In the late 1990s, the KTeV collaboration at Fermilab reported a null result from searches for the spontaneous appearance of $\pi^+\pi^-$ pairs, or a single π^0 consistent with the decay of a long-lived neutral particle produced by 800 GeV protons on a beryllium target. They excluded the interesting range $m_{R^0} \sim$ 1–3 GeV for a lifetime between 3×10^{-10} and 10^{-3} s.

These experimental results leave little if any room for light gluinos with mass less than 5–10 GeV. When combined with limits from UA1 and UA2, it seems clear that $m_{\tilde{g}} \gtrsim 79$ GeV.

15.2 Search for SUSY at LEP and LEP2

In 1989, the CERN Large Electron Positron collider (LEP) began operating at and around the Z pole, $\sqrt{s} \simeq 91$ GeV. Data was collected at the Z pole by the four experiments ALEPH, DELPHI, L3 and OPAL through 1995. At that point, each experiment had accumulated over 4 million Z boson events, corresponding to an integrated luminosity of over 150 pb^{-1}. In 1995, the center of mass collider energy was raised to 136 GeV, and over subsequent years it was raised beyond WW and ZZ thresholds until a maximum energy of $\sqrt{s} \simeq 208$ GeV was reached in the year 2000, in an effort to flush out the Higgs boson.

15.2.1 SUSY searches at the Z pole

The four LEP experiments together accumulated a sample of about 17M Z^0 events allowing very precise determination of the Z^0 line-shape. In particular, $\Delta\Gamma_Z$ as well as $\Delta\Gamma_{\text{inv}}$, the non-SM contributions to the total and "invisible" widths of the

https://doi.org/10.1017/9781009289801.016 Published online by Cambridge University Press

Z^0, are constrained to be smaller than a few MeV. The former leads to lower limits only slightly below $M_Z/2$ on masses of MSSM sparticles ($\tilde{f}$, $\widetilde{W}_i$) with significant couplings to Z^0. This limit is *independent* of the decay properties of the sparticles. The limit $\Delta\Gamma_{\rm inv} < 2$ MeV strongly constrains the partial width for Z decays to $\widetilde{Z}_1$ pairs, but does not lead to a model-independent lower limit on $m_{\widetilde{Z}_1}$ because of the strong parameter dependence of the $Z\widetilde{Z}_1\widetilde{Z}_1$ coupling. The invisible width puts a bound very close to $M_Z/2$ on (quasi-)stable or invisibly decaying sneutrinos.

The large number of Z^0 boson events also gave lower limits essentially equal to $M_Z/2$ on $m_{\widetilde{W}_1}$, $m_{\tilde{q}_{\rm L,R}}$, and $m_{\tilde{\ell}_{\rm L,R}}$. These limits, which come from searches for final state configurations with low SM backgrounds, depend on how the sparticles decay, and so are somewhat model-dependent. These limits would be evaded if the parent sparticle had a mass close to the daughter LSP so that the visible decay products are very soft. Alternatively, limits on $\tilde{t}_1$ or $\tilde{b}_1$ masses could be evaded for values of the squark mixing angle such that the corresponding Z partial width is very small.

Searches for $Z^0 \to \widetilde{Z}_1\widetilde{Z}_2 \to \widetilde{Z}_1 + f\bar{f}\widetilde{Z}_1$ are of special interest because this reaction, which leads to distinctive events with acolinear leptons or jets and large missing transverse energy, may be kinematically accessible even if $Z \to \widetilde{W}_1^+\widetilde{W}_1^-$ is not. Unfortunately, the $Z\widetilde{Z}_i\widetilde{Z}_j$ coupling is very parameter-dependent, and vanishes if either neutralino is a gaugino. Even so the LEP experiments, which are able to exclude branching fractions for $Z \to \widetilde{Z}_1\widetilde{Z}_2$ larger than $(2-20)\times 10^{-6}$ (depending on the values of the neutralino masses), are able to exclude regions of parameter space that would otherwise not be accessible.

15.2.2 SUSY searches at LEP2

All four LEP experiments collected data for several center of mass energies ranging from $\sqrt{s} = M_Z$ up to $\sqrt{s} = 203$–208 GeV, where each experiment accumulated over 210 pb^{-1} of integrated luminosity. Non-observation of any signal in a large number of final states was interpreted as lower limits on many sparticle masses. The precise limits are somewhat model-dependent but, because of the clean experimental environment, are frequently close to the kinematic limit. We summarize these limits in Table 15.1.

Charged sleptons are searched for assuming that these decay via $\tilde{\ell} \to \ell\widetilde{Z}_1$, and that the neutralino LSP escapes detection. Since the cross section for selectron pair production is considerably larger than that for smuon or stau production, the limits on $m_{\tilde{e}_{\rm R}}$ are somewhat stronger. The limit on $m_{\tilde{\tau}_1}$ also depends on θ_τ. Since third generation squarks are expected to be lighter than squarks of other generations, LEP2 experiments focussed on searches for $\tilde{t}_1$ and $\tilde{b}_1$ squarks. The limits obtained depend on the corresponding mixing angle as well as on their assumed decay patterns. Experiments at LEP2 have also searched for charginos produced via

https://doi.org/10.1017/9781009289801.016 Published online by Cambridge University Press

Table 15.1 *Limits on various sparticle masses from the non-observation of any signal in experiments at LEP2. The limits on $m_{\tilde{t}_1}$ ($m_{\tilde{b}_1}$) are shown for two cases of squark mixing angle: no mixing, and mixing such that the coupling to Z^0 vanishes. The limit on the chargino mass for small mass gaps is obtained from a combination of results including searches for soft events with radiated photons from the initial state, for long-lived particles that manifest themselves by tracks with kinks or impact parameter off-sets, or for quasi-stable heavy charged particles.*

sparticle	mass bound (GeV)	comment
$\tilde{e}_R$	99	$\tilde{e}_R \to e\widetilde{Z}_1$, $\Delta m > 10$ GeV
$\tilde{\mu}_R$	94	$\tilde{\mu}_R \to \mu\widetilde{Z}_1$, $\Delta m > 10$ GeV
$\tilde{\tau}_1$	85	$\tilde{\tau}_R \to \tau\widetilde{Z}_1$, $\Delta m > 10$ GeV
$\tilde{t}_1$	98 (94)	$\tilde{t}_1 \to c\widetilde{Z}_1$, $\Delta m > 10$ GeV, $\theta_t = 0(56^\circ)$
$\tilde{t}_1$	99 (95)	$\tilde{t}_1 \to b\ell\tilde{\nu}_L$, $\Delta m > 10$ GeV, $\theta_t = 0(56^\circ)$
$\tilde{b}_1$	99 (95)	$\tilde{b}_1 \to b\widetilde{Z}_1$, $\Delta m > 10$ GeV, $\theta_b = 0(68^\circ)$
$\widetilde{W}_1$	103.5	$m_{\tilde{\nu}_e} > 300$ GeV, $\Delta m > 10$ GeV, gaugino mass unification
$\widetilde{W}_1$	91.9	$m_{\tilde{\nu}_e} \sim 500$ GeV

$e^+e^- \to \widetilde{W}_1\overline{\widetilde{W}}_1$, followed by $\widetilde{W}_1 \to f\bar{f}'\widetilde{Z}_1$, where f and f' are quarks or leptons. The signature channels include: (i) four-jet $+E^{\text{miss}}$ events, (ii) lepton + two-jets $+E^{\text{miss}}$ events, and (iii) lepton–antilepton $+E^{\text{miss}}$ events, where E^{miss} denotes the apparent missing energy in the event. Since the production cross section is not suppressed by the p-wave β^3 factor as for scalar pair production, the experimental limit is usually very close to the phase space boundary. Exceptions occur either when $m_{\widetilde{W}_1} - m_{\widetilde{Z}_1}$ is very small so that the energy of the visible decay products and the momentum carried off by the LSP are both small, or when the sneutrino is rather light and the contribution of the t-channel sneutrino exchange to the production amplitude (which interferes destructively with the s-channel contributions) is significant. Neutralino pair production was also searched for in the $e^+e^- \to \widetilde{Z}_1\widetilde{Z}_2$, $\widetilde{Z}_2\widetilde{Z}_2$ channels, where $\widetilde{Z}_2 \to \widetilde{Z}_1 + f\bar{f}$. The production cross sections and decay branching fractions are very parameter dependent, and no model-independent limit on neutralino masses can be extracted. Nonetheless, upper limits on the cross section for various event topologies restrict the parameter space of various models of MSSM sparticle masses.

Searches within mSUGRA

Many SUSY searches have been carried out within the mSUGRA framework, or the MSSM with additional assumptions about degeneracy of sfermions. The limits

https://doi.org/10.1017/9781009289801.016 Published online by Cambridge University Press

in Table 15.1 for $\Delta m > 10$ GeV are essentially those that would be obtained in mSUGRA. However, because this framework is very constrained, the limits on the chargino mass together with those on neutralino production cross sections imply a limit $m_{\widetilde{Z}_1} > 50$ GeV on the neutralino LSP for any set of mSUGRA parameters. This serves as an example of the interplay between collider experiments and searches for relic dark matter.

Searches within the mGMSB model

We have seen that SUSY signals may differ from those in the MSSM if the LSP is an ultra-light gravitino as may be the case within the mGMSB framework. In this case, searches would naturally focus on the next-to-lightest SUSY particle (NLSP) which, depending on n_5, is either $\tilde{\tau}_1$ or the neutralino. The search strategy depends on the lifetime of the NLSP which, as we have seen, can vary over a wide range, depending on the gravitino mass. For the stau NLSP scenario, the negative result of the search for acoplanar tau pairs without any displaced vertices implies $m_{\tilde{\tau}_1} > 87$ GeV. If the stau is very long-lived so that it decays outside the detector, searches for heavy stable charged particles imply $m_{\tilde{\tau}_1} > 97$ GeV, while for intermediate lifetimes, searches for tracks with large impact parameters or tracks with kinks lead to a mass bound somewhere in between. For the co-NLSP case, corresponding searches imply $m_{\tilde{\mu}_R} > 96$ GeV, independent of the smuon lifetime.

For the case of a neutralino LSP decaying outside the detector, sparticle masses are bounded as in Table 15.1. Stronger bounds can be obtained if the neutralino decays via $\widetilde{Z}_1 \to \gamma \tilde{G}$ within the detector. Since the neutralino pair production cross section depends on the selectron mass, the limit obtained depends on n_5.[1] For $m_{\tilde{e}_R} = 1.1 m_{\widetilde{Z}_1}(2m_{\widetilde{Z}_1})$ (this covers the range $n_5 = 1$–4) the negative results of a search for acolinear photon pairs at LEP2 implies that $m_{\widetilde{Z}_1} \gtrsim 92(96)$ GeV.

Searches within the AMSB model

In AMSB models, the chargino $\widetilde{W}_1$ and neutralino $\widetilde{Z}_1$ are expected to be nearly mass degenerate and, as discussed in Section 13.4.1, the visible decay products from chargino decay are very soft. In this case, the bound $m_{\widetilde{W}_1} > 91.9$ GeV in the last row of Table 15.1 applies since the sneutrino is typically quite heavy in this scenario.

15.2.3 SUSY Higgs searches at LEP2

The search for neutral Higgs scalars is especially interesting in the SUSY context because $m_h \lesssim 130$ GeV within the MSSM, and a Higgs boson in this mass range is

[1] Recall though that $\widetilde{Z}_1$ is typically the NLSP only for $n_5 = 1$.

https://doi.org/10.1017/9781009289801.016 Published online by Cambridge University Press

what is expected from a global fit of LEP and other electroweak data to the SM.[2] A lighter Higgs boson h, within the kinematic reach of LEP2, could have been produced via

$$e^+e^- \to Zh \text{ or } Ah \tag{15.4}$$

processes, both of which occur via s-channel Z^0 exchange. Moreover, the two reactions are complementary in the sense that the ZZh and the ZAh coupling cannot both simultaneously vanish (at tree level). The first of these reactions is also the usual process for searching for the SM Higgs boson. While h and A are expected to dominantly decay into $b\bar{b}$ pairs, a variety of final states is possible, including the one with an "invisible h" if the decay $h \to \widetilde{Z}_1\widetilde{Z}_1$ is allowed.

Shortly before the termination of the LEP2 collider, an excess of events in the four-jet sample with displaced vertices and a "$b\bar{b}$ mass" ~ 114 GeV caused some excitement. However, a final dedicated run of LEP around $\sqrt{s} = 208$ GeV did not unearth any signal and a limit,

$$m_{H_{\rm SM}} > 114.3 \text{ GeV}, \tag{15.5}$$

was obtained on the SM Higgs boson mass. Assuming CP is conserved in the Higgs sector, the same bound also applies to m_h for large values of m_A. However, the LEP collaborations also performed dedicated analyses to search for MSSM Higgs bosons in several channels, but found no signal. Since the masses and couplings of the Higgs bosons to SM particles are determined at tree level by $\tan\beta$ together with any *one* of the physical particle masses (taken to be m_A in Chapter 8), the results of these searches can be conveniently displayed in the $m_A - \tan\beta$ plane as shown in Fig. 15.1. Once radiative corrections are included, the Higgs sector depends also on other SUSY parameters: the excluded region shown is conservative in the sense that SUSY parameters are chosen to maximize m_h for a given value of $\tan\beta$.

15.3 Supersymmetry searches at the Tevatron

The Collider Detector at Fermilab (CDF) and DØ are the major general purpose experiments at the Fermilab Tevatron $p\bar{p}$ collider. During Run 1, when each of these experiments accumulated an integrated luminosity of $\sim 100\,\text{pb}^{-1}$ at $\sqrt{s} = 1.8$ TeV, the top quark was discovered and its mass determined to be $m_t = 174.3 \pm 5.1$ GeV. The experiments also searched for new physics, albeit with null results. Run 2 of the Tevatron began in 2001 at $\sqrt{s} \simeq 2$ TeV, featuring the Tevatron Main Injector along with upgraded detectors designed to handle the large increase in beam luminosity.

[2] If we assume that all couplings remain perturbative out to a very high energy scale, we obtain a model-independent bound $m_h \lesssim 160$ GeV as long as SUSY is broken at the weak scale, to be compared with the corresponding bound of about 200 GeV on the SM Higgs boson mass.

https://doi.org/10.1017/9781009289801.016 Published online by Cambridge University Press

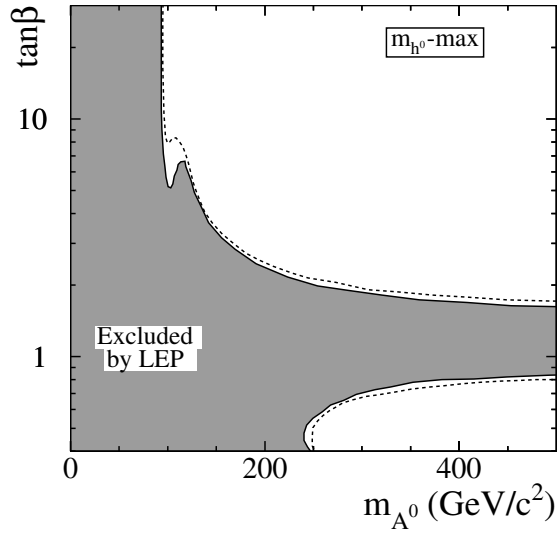

Figure 15.1 The shaded region shows the portion of the $m_A - \tan\beta$ plane excluded by the null results of the searches for MSSM Higgs bosons at LEP2. Here, $M_2 = -\mu = 200$ GeV, $m_{\tilde{g}} = 800$ GeV, all soft SUSY breaking sfermion masses set to 1 TeV and the top squark mixing adjusted to maximize m_h for a given value of $\tan\beta$. The LEP excluded region is sensitive to the value of the top quark mass which is taken to be 179.3 GeV. For this scenario, the LEP data exclude $0.9 \leq \tan\beta \leq 1.5$; this range is also sensitive to the choice of m_t. The dashed lines mark the boundaries of the region that would be expected to be excluded on the basis of Monte Carlo simulations, assuming no signal events. Throughout the analysis, it is assumed that there are no SUSY sources of CP violation. For details of the analysis, see LHWG-Note 2004-01. We thank P. Igo-Kemenes for supplying this figure.

Run 2 is expected to continue at least until 2007 when the CERN LHC pp collider is expected to commence operation. During this run, each experiment is currently expected to accumulate an integrated luminosity of 5–10 fb^{-1}, though higher values were initially anticipated.

15.3.1 Supersymmetry searches at run 1

Searches for gluinos and squarks

The CDF and DØ collaborations have continued the search for squarks and gluinos begun at CERN. The first searches focussed on the multijet $+E_{\mathrm{T}}^{\mathrm{miss}}$ signature from $\tilde{g}\tilde{g}$, $\tilde{g}\tilde{q}$, and $\tilde{q}\tilde{q}$ production, followed by the direct decays of squarks and gluinos to $\widetilde{Z}_1$. It was subsequently realized that, as we saw in Chapter 13, heavier squarks and gluinos are more likely to decay via cascades than to decay directly to the LSP, so that the momentum of the LSPs, and hence the $E_{\mathrm{T}}^{\mathrm{miss}}$, is somewhat degraded. The cascade decay patterns are model-dependent, and the mSUGRA model began

https://doi.org/10.1017/9781009289801.016 Published online by Cambridge University Press

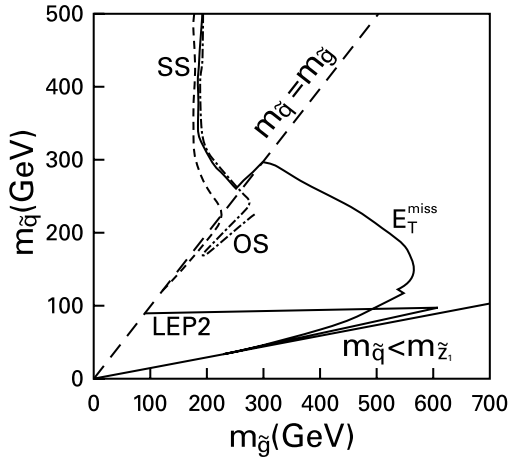

Figure 15.2 The region of the $m_{\tilde{g}} - m_{\tilde{q}}$ plane excluded by various searches for squark and gluino production at the Fermilab Tevatron. The solid contour labeled $E_{\mathrm{T}}^{\mathrm{miss}}$ shows the boundary of the regions excluded by different searches in multijet $+E_{\mathrm{T}}^{\mathrm{miss}}$ channels, while the dashed (dashed-dotted) contours labeled SS (OS) mark the boundaries of the regions excluded by the CDF (DØ) search in the SS dilepton (OS dielectron) channel. We caution that these searches have been performed in somewhat different models, and refer the reader interested in details to the original papers. We note that the dot-dashed contour is our transcription of the original contour that was presented in the $m_0 - m_{1/2}$ plane of the mSUGRA model. Finally, the region marked LEP2 is excluded by searches for squark pair production at LEP2.

to be adopted for many phenomenological analyses. Within this framework, as we have already seen, squarks can never be much lighter than gluinos. The Tevatron collaborations, quite rightly, disregard this model-dependent restriction, and also perform a search for squark production, assuming that the gluino is heavy. For this purpose, they adopt the MSSM with gaugino mass unification, assuming a mass degeneracy for the three generations of squarks.

The analysis of the $E_{\mathrm{T}}^{\mathrm{miss}}$ signal is complicated. To enhance the signal over backgrounds from SM events with neutrinos, or from mismeasurements of jets, carefully designed selection cuts are applied to the data.[3] Moreover, these cuts are optimized, depending on the mass of squarks and gluinos being searched for. The CDF and DØ collaborations have already performed several analyses, using different sets of cuts, but have found no evidence for any excess of events above SM expectations. The region of the $m_{\tilde{g}} - m_{\tilde{q}}$ plane excluded by these searches is summarized by the solid contour labeled $E_{\mathrm{T}}^{\mathrm{miss}}$ in Fig. 15.2. This contour is a composite from several Tevatron searches with different selection cuts. In the upper

[3] These backgrounds mainly come from W and Z production, vector boson pair production (WW, WZ, and ZZ) and heavy flavor production ($c\bar{c}$, $b\bar{b}$, and $t\bar{t}$).

https://doi.org/10.1017/9781009289801.016 Published online by Cambridge University Press

portion of the plane, the analysis is performed within the mSUGRA framework, but for the lower portion (where squarks much lighter than gluinos are not allowed in the mSUGRA model) the MSSM with gaugino mass unification, and ten flavors of degenerate squarks is used. Since different analyses are used for mSUGRA and the MSSM, the excluded region does not match up when $m_{\tilde{q}} = m_{\tilde{g}}$. The reason that the range of $m_{\tilde{q}}$ excluded by the $E_{\rm T}^{\rm miss}$ search cuts off for large values of $m_{\tilde{g}}$ is that the LSP mass increases with $m_{\tilde{g}}$, and the transverse momentum carried off by the LSPs is correspondingly reduced. We see from the figure that within the mSUGRA framework, gluinos lighter than 195 GeV are excluded (95% CL) for any value of $m_{\tilde{q}}$ while, if $m_{\tilde{g}} \simeq m_{\tilde{q}}$, the mass limit extends to as much as 300 GeV, depending on the analysis.

Although cascade decays degrade the reach of CDF and DØ $E_{\rm T}^{\rm miss}$ searches because they soften the $E_{\rm T}^{\rm miss}$ spectrum, they also lead to novel signatures for gluino and squark production. If daughters $\widetilde{W}_1$ and $\widetilde{Z}_2$ decay leptonically, gluino and squark production leads to events with several jets together with n hard, isolated leptons and $E_{\rm T}^{\rm miss}$. Within the SM there is a substantial background from high $p_{\rm T}$ $W \to \ell\nu$ production if $n = 1$ but, for $n \geq 2$, SM backgrounds are rather small. One important background comes from high $p_{\rm T}$ $Z^0 \to \ell^+\ell^-$ events which contain opposite sign lepton pairs with the same flavor. These can be easily vetoed by requiring that the dilepton mass not reconstruct to M_Z within some error. Especially interesting are events with same sign dileptons from gluino pair production that we had mentioned in our discussion just below Eq. (13.9) (these may also come from $\tilde{g}\tilde{q}$ or $\tilde{q}\tilde{q}$ production), or events with $n \geq 3$ leptons because SM backgrounds to these event topologies are very small. The cross section for multilepton topologies is suppressed by branching fractions for leptonic decays of charginos and neutralinos and so requires data samples with significant integrated luminosities to obtain a handful of signal events. The dashed contour labeled SS in Fig. 15.2 shows the region excluded by a CDF search in the same sign dilepton channel, while the dot-dashed contour labeled OS shows the corresponding region from the dielectron analysis by the DØ collaboration. These analyses of course depend on the cascade decay patterns which are somewhat model-dependent. For instance, the OS contour, which was obtained within the mSUGRA model framework, terminates at the boundary of parameter space when $m_0 = 0$, while the wedge in it occurs because cascade decay patterns are altered when sleptons and/or sneutrinos become light enough to be produced as decay products of charginos and neutralinos. Our main point, however, is that these leptonic searches, even with an integrated luminosity of just 100 pb^{-1}, are already competitive with the $E_{\rm T}^{\rm miss}$ search. With the much larger data sample anticipated in Run 2, it may be the case that the rate limited but cleaner same sign dilepton and trilepton event channels will lead to a better reach than the $E_{\rm T}^{\rm miss}$ channel.

Search for charginos and neutralinos

Charginos and neutralinos are produced via electroweak interactions and so have cross sections comparable to those for pair production of W and Z^0 bosons. Signals from their hadronic decays are buried under QCD backgrounds, so that searches are forced to focus on events containing isolated leptons. Signals from $\widetilde{W}_1\widetilde{Z}_1$ production where $\widetilde{W}_1 \to \ell\nu\widetilde{Z}_1$ are buried under background from the resonantly produced $W \to \ell\nu$ decays. Indeed the most promising signal for chargino and neutralino production comes from hadronically quiet (except for jet activity from QCD radiation) isolated trilepton events expected from $(\widetilde{W}_1 \to \ell\nu_\ell\widetilde{Z}_1) + (\widetilde{Z}_2 \to \ell\bar{\ell}\widetilde{Z}_1)$ production. We have already seen in Fig. 12.22 that for models with gaugino mass unification, $\widetilde{W}_1\widetilde{Z}_2$ production may be the dominant production mechanism for SUSY particle production at the Tevatron, and also that if sleptons are sufficiently light, then the $\widetilde{Z}_2$ leptonic branching fraction may be significantly enhanced. Since leptons from $Z^0 \to \ell^+\ell^-$ can be readily identified, the most serious SM background comes from $W(\to \ell\nu_\ell) + Z(\to \tau\bar{\tau})$ followed by leptonic τ decays, and from $W^{(*)}\gamma^*$ and $W^{(*)}Z^{(*)}$ production, where the off-shell vector bosons "decay" leptonically.

Searches for isolated trilepton events from SUSY have been performed by both CDF and DØ for the Run 1 data sample. If the leptonic branching fractions for chargino and neutralino decays are similar to those of the W and Z^0 boson, the chargino mass bound obtained is well below the corresponding LEP2 limit, but exceeds it if leptonic chargino and neutralino decays are enhanced by the presence of light sleptons. These searches are, however, a proof of principle and will yield interesting results when the integrated luminosity levels associated with Run 2 are achieved.[4]

Search for top and bottom squarks

Since third generation squarks are expected to be lighter than other squarks, dedicated searches for these have been performed at the Tevatron by both the CDF and DØ collaborations. If $\tilde{t}_1\bar{\tilde{t}}_1$ production occurs at a large rate at the Tevatron, and $m_{\tilde{t}_1} < m_b + m_{\widetilde{W}_1}$, then $\tilde{t}_1$ is likely to decay dominantly via $\tilde{t}_1 \to c\widetilde{Z}_1$, resulting in a $c\bar{c} + E_{\mathrm{T}}^{\mathrm{miss}}$ final state. For $m_{\widetilde{Z}_1} \lesssim 50$ GeV, the CDF search excludes $m_{\tilde{t}_1}$ up to ~ 110 GeV, extending beyond the reach of LEP2.[5] Searches have also been performed for the case when $\tilde{t}_1 \to b\widetilde{W}_1$. In this case, a reach beyond the current LEP2 bound is obtained only if the leptonic branching fraction of $\widetilde{W}_1$ is large. Assuming that $\widetilde{W}_1 \to \ell\tilde{\nu}$, the combined result of the two collaborations implies that $m_{\tilde{t}_1} \gtrsim 125$–$140$ GeV for $m_{\tilde{\nu}} = 60$–85 GeV and $m_{\widetilde{W}_1}$ beyond the LEP2 bound.

[4] We should also emphasize that chargino and neutralino searches are independent of gluino searches via $E_{\mathrm{T}}^{\mathrm{miss}}$ events, and in models without gaugino mass unification yield completely independent information.

[5] Since $\sigma(\tilde{t}_1\bar{\tilde{t}}_1)$ is completely determined by $m_{\tilde{t}_1}$, this excluded region is completely determined by $m_{\tilde{t}_1}$ and $m_{\widetilde{Z}_1}$, and is independent of other model parameters.

https://doi.org/10.1017/9781009289801.016 Published online by Cambridge University Press

Searches have also been performed for $t\bar{t}$ production where $t \to \tilde{t}_1 \widetilde{Z}_1$ decay assuming $\tilde{t}_1 \to b\widetilde{W}_1 \to b\ell\tilde{\nu}$, but significant bounds on $m_{\tilde{t}_1}$ are obtained only if the branching fraction for the SUSY decay of t is in excess of $\sim 45\%$.

Both the DØ and CDF collaborations have also searched for $p\bar{p} \to \tilde{b}_1\bar{\tilde{b}}_1 X$ production assuming $\tilde{b}_1 \to b\widetilde{Z}_1$. The absence of a signal has been interpreted as an exclusion of a portion of the $m_{\tilde{b}_1}$ *vs.* $m_{\widetilde{Z}_1}$ plane. Values of $m_{\tilde{b}_1} \lesssim 130$ GeV are excluded if $m_{\tilde{b}_1} - m_{\widetilde{Z}_1} \gtrsim 50$–$60$ GeV, and $m_{\tilde{b}_1}$ as large as 145 GeV is excluded for low values of $m_{\widetilde{Z}_1}$.

Searches for SUSY in GMSB models

In GMSB models with a neutralino that decays via $\widetilde{Z}_1 \to \gamma\tilde{G}$ as the NLSP, we would expect sparticle production to lead to $\gamma\gamma + \text{jets} + \text{leptons} + E_{\mathrm{T}}^{\mathrm{miss}}$ events. The DØ collaboration found no excess above SM expectation in their inclusive $\gamma\gamma + E_{\mathrm{T}}^{\mathrm{miss}}$ sample and set a limit $m_{\widetilde{Z}_1} > 77$ GeV, corresponding to $m_{\widetilde{W}_1} > 150$ GeV at the 95% CL. From the null result of a search for gravitino pair production tagged by a high E_{T} jet from the initial state, the CDF collaboration concluded that the gravitino mass must be heavier than about 1.1×10^{-5} eV corresponding to the SUSY breaking scale $\sqrt{F} \geq 215$ GeV.[6] They also concluded that there was no signal in the $\ell + \gamma + E_{\mathrm{T}}^{\mathrm{miss}}$ as well as the b-jet + $E_{\mathrm{T}}^{\mathrm{miss}}$ channels, although there was a small excess in the first of these channels.

15.3.2 Prospects for future SUSY searches

Run 2 of the Fermilab Tevatron began in 2001. Current expectation is that an integrated luminosity of 5–10 fb^{-1} will be expected before the LHC begins to operate, down from 15–25 fb^{-1} that had been originally anticipated. It is interesting to project the SUSY reach of Tevatron experiments for this vastly larger data sample.

The $E_{\mathrm{T}}^{\mathrm{miss}}$ channel

The current limits on charginos from LEP2, that $m_{\widetilde{W}_1} > 103$ GeV given a reasonable mass gap between $\widetilde{W}_1$ and $\widetilde{Z}_1$, imply that $m_{\tilde{g}} \gtrsim 330$–$400$ GeV (depending on the sign of μ) in models with gaugino mass unification, if $\tan\beta \gtrsim 1.5$ as suggested by Fig. 15.1. As already mentioned, in addition to the $E_{\mathrm{T}}^{\mathrm{miss}}$ signal, multilepton signals are also potentially important. The size of these signals is sensitive to which sparticles are dominantly produced, and on how they decay, and so are model-dependent. The $E_{\mathrm{T}}^{\mathrm{miss}}$ signal is somewhat more robust.

In Fig. 15.3, we show regions of mSUGRA parameter space where the somewhat more robust $E_{\mathrm{T}}^{\mathrm{miss}}$ + jets signal ought to be visible above SM backgrounds at at least

[6] Recall from our discussion of goldstino interactions that this cross section is fixed by the gravitino mass.

https://doi.org/10.1017/9781009289801.016 Published online by Cambridge University Press

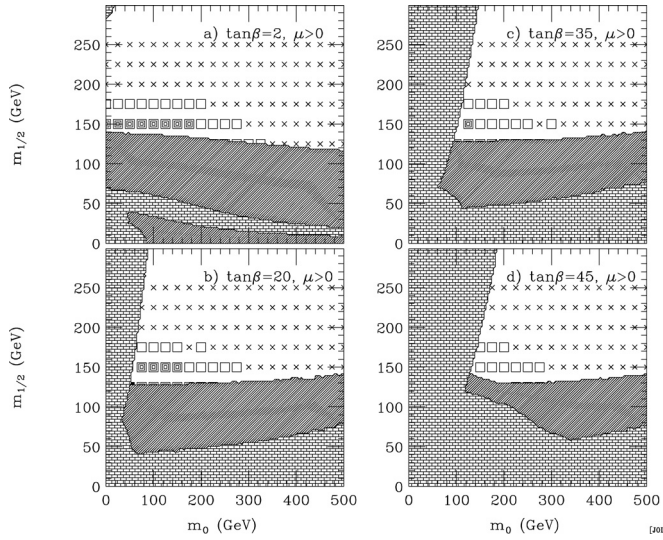

Figure 15.3 A plot of points accessible at 5σ level at Tevatron Run 2 for 2 fb^{-1} (gray squares) and 25 fb^{-1} (white squares) of data in searches for mSUGRA via $E_{\mathrm{T}}^{\mathrm{miss}}$+ multijet events. Points with a $\times$ symbol are inaccessible at Run 2 via the $E_{\mathrm{T}}^{\mathrm{miss}}$ + jets signal. Reprinted with permission from H. Baer, C. H. Chen, M. Drees, F. Paige and X. Tata, *Phys. Rev.* **D58**, 075008 (1998), copyright (1998) by the American Physical Society.

the 5σ level. The bricked areas are disallowed by a lack of radiative EWSB (low $m_{1/2}$ region) or a charged (slepton) LSP (low m_0 region). The hatched region is excluded by LEP2 searches. The gray squares denote model points where a 5σ signal is expected with 2 fb^{-1} of data, while points denoted by open squares are accessible only for an integrated luminosity of 25 fb^{-1}. We stress that, although it appears that the LEP limit on the chargino excludes much of the parameter plane accessible to experiment, this $E_{\mathrm{T}}^{\mathrm{miss}}$ search is still important because it can probe squark and gluino masses without any assumption about gaugino mass unification.

Multilepton channels

Tevatron experiments have already shown that searches via multilepton + $E_{\mathrm{T}}^{\mathrm{miss}}$ events are competitive with the traditional $E_{\mathrm{T}}^{\mathrm{miss}}$ search. The signals can naturally be sorted according to the number of isolated leptons contained in each event: $E_{\mathrm{T}}^{\mathrm{miss}}$ + jets, $1\ell + E_{\mathrm{T}}^{\mathrm{miss}}$+ jets, opposite sign (OS) or same sign (SS) dileptons + $E_{\mathrm{T}}^{\mathrm{miss}}$ + jets and $3\ell + E_{\mathrm{T}}^{\mathrm{miss}}$ + jets. We will focus our attention on the trilepton signal which, for large data samples, yields the largest reach in models with gaugino mass unification. Here, we focus on this signal within the mSUGRA framework, but it should be kept in mind that both OS and SS dilepton signals may also be observable.

https://doi.org/10.1017/9781009289801.016 Published online by Cambridge University Press

Within the mSUGRA framework, LEP bounds imply that $\widetilde{W}_1\widetilde{Z}_2$ and $\widetilde{W}_1\widetilde{W}_1$ production have the largest sparticle production cross sections at the Tevatron if SUSY is accessible at all. It makes sense to focus on the trilepton signals arising from the former reaction since these have rather low SM backgrounds. The background size can be gauged from the fact that the inclusion of backgrounds from $W^{(*)}\gamma^*$ and $W^{(*)}Z^*$ sources of trileptons is important.

It might seem that the signal appears as trilepton events free from jet activity. Detailed studies, however, show that the largest reach is obtained in the inclusive trilepton channel after suitable cuts, since the production of heavy sparticles is frequently associated with jets from initial state QCD radiation. Moreover, gluino and squark production, which leads to jetty trilepton events, also makes a subdominant contribution to this signal.

For small to intermediate values of $\tan\beta$, the leptons from chargino and neutralino decays are relatively hard and readily detectable. We have seen in Chapter 13 that if $\tan\beta$ is large, decays to third generation leptons and neutrinos are enhanced at the expense of those to the experimentally detectable e and μ. For large $\tan\beta$, the leptons in the $\ell\ell\ell'$ signal (ℓ, $\ell' = e$, μ) arise as secondary daughters from τ decay, and so tend to be soft. It was shown, however, that using a special set of soft lepton cuts, the trilepton signal should be detectable above backgrounds over a wide range of $\tan\beta$.[7]

The region of the m_0 vs. $m_{1/2}$ plane where the trilepton signal is observable at the Tevatron is illustrated in Fig. 15.4 for a moderate and a high value of $\tan\beta$. The dark shaded region on the left is excluded because the stau is the LSP, while the right-hand side is excluded because electroweak symmetry is improperly broken, since $\mu^2 < 0$. Just to the left of this latter boundary, μ^2 is small, and $m_{\widetilde{W}_1} \sim m_{\widetilde{Z}_1} \sim |\mu|$. For small $m_{1/2}$, this is the so-called focus point (FP) region, while for larger $m_{1/2}$ values this has been referred to as the hyperbolic branch (HB).

The light-shaded region is excluded by constraints from LEP2. Below the band, $m_h < 114.1$ GeV. Below the solid (dashed) contours, Tevatron experiments should be able to see the trilepton signal at the 5σ (3σ) level with an integrated luminosity of 10 (25) fb^{-1}. For the $\tan\beta = 10$ case, we see a large signal at low values of m_0 for which charginos and neutralinos decay into real sleptons, so that their leptonic branching ratio is nearly 100%. In this case, the reach extends to $m_{1/2}$ as high as 240–260 GeV. As m_0 increases, these decays are no longer kinematically accessible, and the reach drops sharply. For $m_0 \sim 200$ GeV, $B(\widetilde{Z}_2 \to \ell\bar{\ell}\widetilde{Z}_1)$ is very small because of the negative interference between the Z and slepton-mediated amplitudes for $\widetilde{Z}_2$ decay and there is no reach via this channel. As m_0 is increased further, the

[7] See, e.g., S. Abel *et al.*, Report of the SUGRA Working Group at the *Physics at Run II: SUSY and Higgs Workshop*, hep-ph/0003154, and references cited therein.

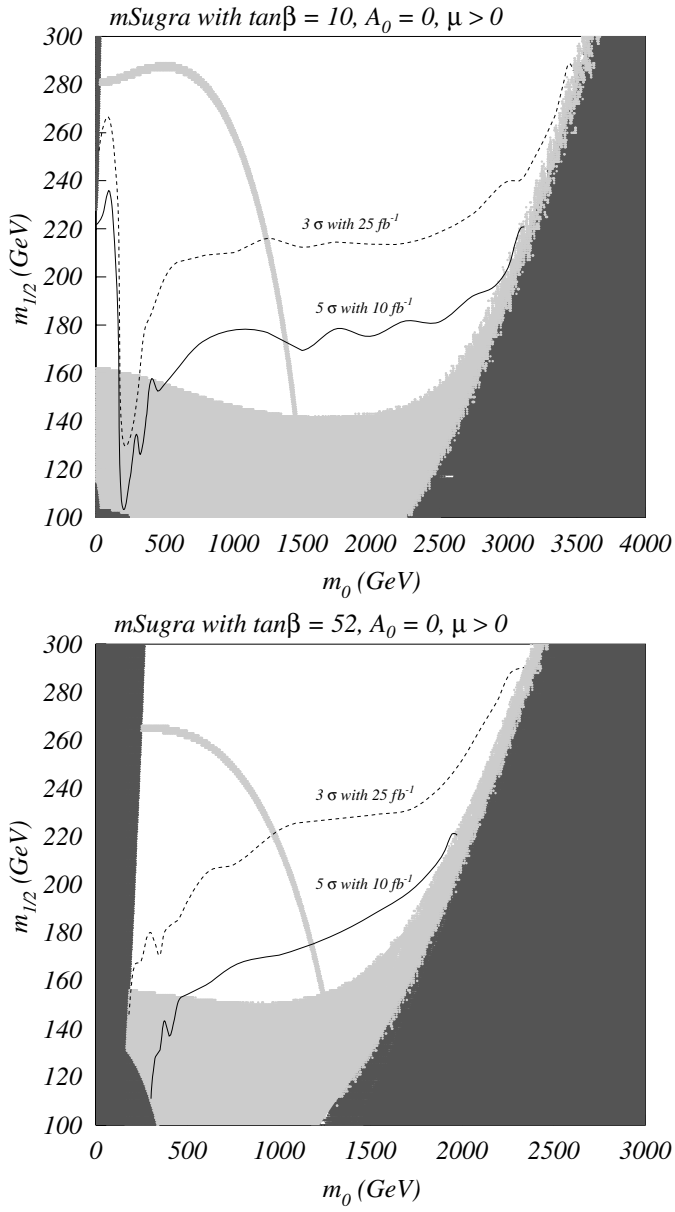

Figure 15.4 The region of the $m_0 - m_{1/2}$ plane where the inclusive trilepton signal with soft leptons is detectable at Tevatron Run 2. The dark-shaded region is excluded by theoretical constraints discussed in the text, while the light-shaded region is excluded by experimental constraints from LEP2. Below the thick light gray line, $m_h < 114.1$ GeV. Reprinted from H. Baer, T. Krupovnickas and X. Tata, *JHEP* **07**, 020 (2003).

https://doi.org/10.1017/9781009289801.016 Published online by Cambridge University Press

slepton-mediated amplitudes become unimportant, and the leptonic branching ratio of $\widetilde{Z}_2$ becomes equal to that of the Z^0 boson, and the contours level off. Finally, for very large values of m_0, we enter the HB/FP region and the chargino becomes increasingly higgsino-like and light, and the contours extend to larger values of $m_{1/2}$. It is important to note that the signal becomes difficult to see because the mass gap between $\widetilde{W}_1$ or $\widetilde{Z}_2$ and the LSP becomes small, and the visible decay products become too soft to pass the experimental cuts. A signal might escape detection even if charginos and neutralinos are well within the kinematic reach of the Tevatron. For larger values of $\tan\beta$, the small m_0 region where the trilepton signal is observable shrinks because the chargino preferentially decays to staus, until this region completely disappears as illustrated for $\tan\beta = 52$ in the second frame of Fig. 15.4. Once again the contours rise in the HB/FP region where the chargino becomes relatively light.

The trilepton signal is important from another point of view. Since the like flavor, opposite sign lepton pair in an $\ell^+\ell^-\ell'^{\pm}$ event arises from $\widetilde{Z}_2 \to \ell^+\ell^-\widetilde{Z}_1$ decay, the $m(\ell^+\ell^-)$ distribution must kinematically be bounded by $m_{\widetilde{Z}_2} - m_{\widetilde{Z}_1}$. If the trilepton signal is sufficiently large, it will be possible to determine this dilepton edge which would then serve as a starting point for reconstructing SUSY particle masses.

Top and bottom squarks

Bottom squark pair production can be searched for at CDF and DØ via the $p\bar{p} \to \tilde{b}_1\bar{\tilde{b}}_1 X \to b\bar{b} + E_{\mathrm{T}}^{\mathrm{miss}}$ reaction. Values of $m_{\tilde{b}_1} \sim 210$ (245) GeV can be probed with 2 (25) fb^{-1} of data, assuming $\tilde{b}_1 \to b\widetilde{Z}_1$, and a large $m_{\tilde{b}_1} - m_{\widetilde{Z}_1}$ mass gap. If $\tilde{b} \to b\widetilde{Z}_2$ also occurs at a significant rate, then the reach will be reduced, but this degradation is typically smaller than 30–40 GeV.

The reaction $p\bar{p} \to \tilde{t}_1\bar{\tilde{t}}_1 X$ followed by $\tilde{t}_1 \to b\widetilde{W}_1$ can be searched for at Run 2 in the $b\bar{b}\ell\nu_\ell q\bar{q}'$ final state, which also occurs in direct $t\bar{t}$ production. This search was not possible at Run 1 due to low cross sections and large backgrounds. Mass values of $m_{\tilde{t}_1} \sim 160$–190 GeV can be probed with 2–20 fb^{-1} of data.

If instead $\tilde{t}_1 \to c\widetilde{Z}_1$ is the dominant decay mode, then the Run 1 search for $c\bar{c} + E_{\mathrm{T}}^{\mathrm{miss}}$ final states can be extended. It is estimated that $m_{\tilde{t}_1} \gtrsim 200$ GeV may be probed in 20 fb^{-1}. Alternatively, if $\tilde{t}_1 \to b\ell\tilde{\nu}_\ell$ dominates, then $m_{\tilde{t}_1}$ as large as 240 GeV can be explored if $m_{\tilde{\nu}}$ is as low as 45 GeV.

Search for SUSY Higgs bosons

One of the most intriguing predictions in the MSSM is that the scalar h is lighter than about 135 GeV. This is in the range favored by analyses of electroweak radiative corrections, and possibly within range of discovery at CDF and DØ. Indeed the lack of any excess of $p\bar{p} \to \phi b\bar{b} \to b\bar{b}b\bar{b}$ events ($\phi = h$, H or A) in their data sample has already allowed the CDF collaboration to exclude a portion of the $m_A - \tan\beta$

https://doi.org/10.1017/9781009289801.016 Published online by Cambridge University Press

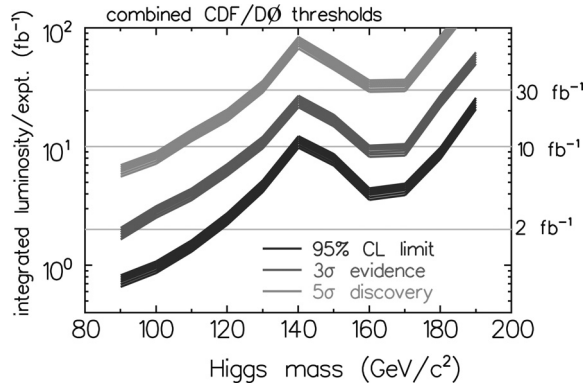

Figure 15.5 Projections for the integrated luminosity required per experiment after combining the data from the CDF and DØ experiments to detect/exclude a SM-like Higgs boson via the channels discussed in the text for a Higgs mass smaller than 130 GeV. For heavier Higgs bosons, not relevant to our discussion, other channels are used. This figure appears in M. Carena *et al.*, Report of the Tevatron Higgs Working Group, FERMILAB-CONF-00-279-T.

plane in Fig. 15.1 with $\tan\beta \geq 50$–100 for values of m_A not excluded at LEP2. The most important reaction for searching for h at the Tevatron is

$$p\bar{p} \to WhX, \quad W \to \ell\nu_\ell, \quad \text{and} \quad h \to b\bar{b}. \tag{15.6}$$

The signal is an isolated lepton together with two b-jets and $E_{\rm T}^{\rm miss}$, where the b-jets are tagged by displaced vertices owing to the long B meson lifetime. The major SM backgrounds come from $Wb\bar{b}$ and $t\bar{t}$ production. The signal is not large, but can be enhanced relative to background because the jet–jet mass is expected to cluster around m_h. Its statistical significance is sensitive to the efficiency for b-tagging and the jet–jet mass resolution that will be attained. This significance can be further enhanced by including signals in other event topologies from Zh, $t\bar{t}h$, and $b\bar{b}h$ production. The results of a detailed analysis (including neural net improvement) of the integrated luminosity required per experiment, after combining the signals in the $\ell b\bar{b} + E_{\rm T}^{\rm miss}$, $b\bar{b} + E_{\rm T}^{\rm miss}$, and $b\bar{b}\ell^+\ell^-$ channels, is shown in Fig. 15.5 for a SM Higgs boson.[8]

One striking implication of Fig. 15.5 is that given an integrated luminosity of 30–40 fb^{-1}, Tevatron experiments would have an excellent chance of discovering h, or apparently ruling out the MSSM. We should, however, be careful before jumping to such a strong conclusion. First, the upper bound on m_h depends on assumptions about how large third generation squark masses and A-parameters might be. Second,

[8] See M. Carena *et al.*, Report of the Tevatron Higgs Working Group, *Physics at Run II: Supersymmetry/Higgs Workshop,* hep-ph/0010338.

https://doi.org/10.1017/9781009289801.016 Published online by Cambridge University Press

the reach shown in these plots depends on projections for jet–jet mass resolutions and b-tagging efficiencies during Run 2. In addition, recent projections indicate that Tevatron experiments will accumulate an integrated luminosity of 5–10 fb^{-1}, in which case the reach is considerably smaller. In this case, tantalizing 3σ effects may be observable if $m_h \lesssim 125$ GeV.

It is worth noting that other neutral Higgs bosons may be accessible to Tevatron searches if $\tan\beta$ is very large. Because the bottom Yukawa coupling increases with $\tan\beta$, the reactions

$$p\bar{p} \to Ab\bar{b}X,\ Hb\bar{b}X \tag{15.7}$$

may probe m_A as large as 160–200 GeV, with 25 fb^{-1} of data. Charged Higgs bosons are generally more difficult to detect.

GMSB models

If an ultra-light gravitino is the LSP, SUSY signals at colliders are sensitive to the identity of the NLSP, which is either the neutralino or the lighter stau (possibly with other sleptons essentially degenerate with the stau) within the mGMSB framework. The decay of the NLSP leads to isolated photons, leptons, or even Z^0 and Higgs bosons, as we saw in Section 13.8.2, in addition to jets, leptons, and $E_{\mathrm{T}}^{\mathrm{miss}}$ expected within the MSSM. Moreover, the NLSP decay may be either prompt or delayed: the latter leads to a variety of novel handles for enhancing the SUSY signal. These include: displaced vertices, tracks with kinks, and tracks corresponding to charged quasi-stable heavy exotics, in addition to the visible daughters from NLSP decays.

In order to assess the Tevatron reach for GMSB models, it is expedient to analyze various "model lines" characterized by the decay properties of the NLSP. For each of these model lines, the reach is evaluated in terms of Λ (which can then be translated to the mass of any sparticle, for instance, the gluino), assuming that the NLSP decays promptly. This is a conservative assumption since delayed decays would serve to enhance the reach. All the model lines have $M = 3\Lambda$ and $C_{\mathrm{grav}} = 1$, and are characterized by:

- **A**. A bino-like NLSP that mainly decays via $\widetilde{Z}_1 \to \gamma\tilde{G}$, for model parameters $n_5 = 1$, $\tan\beta = 2.5$, and $\mu > 0$. SUSY events typically contain two isolated photons in addition to jets, leptons, and $E_{\mathrm{T}}^{\mathrm{miss}}$.
- **B**. A stau NLSP in models with $n_5 = 2$, $\tan\beta = 15$, and $\mu > 0$. In this case, sparticles cascade decay to $\tilde{\tau}_1$, which then decays via $\tilde{\tau}_1 \to \tau\tilde{G}$.
- **C**. A stau–selectron–smuon co-NLSP for model parameters $n_5 = 3$, $\tan\beta = 3$, and $\mu > 0$. SUSY events are then expected to be rich in relatively easily detectable leptons from the decay of the NLSPs in this scenario.

https://doi.org/10.1017/9781009289801.016 Published online by Cambridge University Press

- **D**. A higgsino-like NLSP model line where the NLSP mainly decays via $\widetilde{Z}_1 \to h\tilde{G}$ as long as it is not kinematically suppressed. This does not occur in the mGMSB model where the NLSP tends to be bino-like. However, since the signals are so sensitively dependent on the decay of the NLSP, it is worthwhile to explore this non-canonical scenario and study just how the reach of Tevatron experiments is affected.[9] The model line examined has $n_5 = 2$, $\tan\beta = 3$ with $\mu = -\frac{3}{4}M_1$ to obtain a light higgsino. The Higgs boson yields SUSY events rich in b-jets.
- **E**. A higgsino-like NLSP which dominantly decays via $\widetilde{Z}_1 \to Z^0\tilde{G}$ as long as the decay is not kinematically suppressed. It has the same parameters as model line **D**, except that $\mu = +\frac{3}{4}M_1$.

The reach of the Fermilab Tevatron for an integrated luminosity of 25 fb^{-1} is summarized in Table 15.2 where, in addition to the reach in Λ, we have shown the corresponding value of $m_{\tilde{g}}$ to compare with the reach in other models. We have also listed the event topology that yields the largest reach. We stress again that the reach shown is conservative in that if the NLSP has a long lifetime, the reach may be significantly larger. For instance, by searching for highly ionizing tracks from $\tilde{\tau}_1$ in model line **B**, or tracks with displaced kinks if $\tilde{\tau}_1$ decays within the detector but far from the production point, Λ values as high as ~ 85 TeV can be probed for 30 fb^{-1} of data.

15.4 Supersymmetry searches at supercolliders

The CERN LHC pp collider is scheduled to begin operation in 2007, at $\sqrt{s} \simeq 14$ TeV. Initial runs are expected to accumulate 10 fb^{-1} of integrated luminosity, while several hundred fb^{-1} of data are ultimately expected to be recorded. For gluino and squark masses smaller than ~ 1 TeV, we can see from Fig. 12.14 that several hundred thousand SUSY events would be expected in this data sample!

There is a developing consensus in the high energy physics community that the next big accelerator project should be an electron–positron linear collider operating at a center of mass energy $\sqrt{s} = 500$ GeV which would be upgradeable to $\sqrt{s} =$ 0.8–1 TeV in the second stage. At the start of Section 12.2 we have already discussed the special advantages of these machines for studying new physics, and also the sense in which these could complement the data from the LHC.

In a discussion of supersymmetry at supercolliders, we need to address two conceptually distinct issues.

[9] It is worth noting that additional interactions needed to generate μ and $B\mu$ in this framework could alter the relation between μ and the gaugino masses making such a scenario more plausible.

https://doi.org/10.1017/9781009289801.016 Published online by Cambridge University Press

Table 15.2 *A comparison of the SUSY reach of the Tevatron luminosity upgrade and the LHC for the various model lines of the GMSB framework that were introduced in the text, with the reach in the mSUGRA and AMSB models. For the GMSB model lines, we also show the dominant decay of the NLSP together with the channel that yields the largest reach. For the mSUGRA model, a significantly higher reach in $m_{\tilde{g}}$ is possible, both at the Tevatron as well as at the LHC, if $m_0 \ll m_{1/2}$. For the mAMSB model, the corresponding reach is also larger when m_0 is smaller than in the case that is shown. Studies of the Tevatron reach within the AMSB model are not available.*

Model line	NLSP	Tevatron ($25\ \text{fb}^{-1}$)	LHC ($10\ \text{fb}^{-1}$)
A	$\tilde{Z}_1 \sim \tilde{B}$ $\tilde{Z}_1 \to \gamma\tilde{G}$	$\Lambda \cong 115$ TeV, $m_{\tilde{g}/\tilde{q}} \sim 0.87$ TeV, $ll\gamma\gamma + E_{\text{T}}^{\text{miss}}$	$\Lambda \cong 400$ TeV $m_{\tilde{g}/\tilde{q}} \sim 2.8$ TeV, $\gamma\gamma + E_{\text{T}}^{\text{miss}}$
B	$\tilde{\tau}_1$	$\Lambda \cong 53$ TeV, $m_{\tilde{g}/\tilde{q}} \sim 0.82$ TeV, Clean channels $3l + 1\tau 2l + 1\tau 3l$ $+2\tau 1l + 3\tau 2l$	$\Lambda \cong 150$ TeV $m_{\tilde{g}/\tilde{q}} \sim 2.0$ TeV, $3l + E_{\text{T}}^{\text{miss}}$
C	$\tilde{\tau}_1, \tilde{e}_{\text{R}}, \tilde{\mu}_{\text{R}}$	$\Lambda \cong 60$ TeV, $m_{\tilde{g}/\tilde{q}} \sim 1.3$ TeV, $\geq 4l + E_{\text{T}}^{\text{miss}}$	$\Lambda \cong 155$ TeV $m_{\tilde{g}/\tilde{q}} \sim 3.0$ TeV, $4l + E_{\text{T}}^{\text{miss}}$
D	$\tilde{Z}_1 \sim \tilde{h}$ $\tilde{Z}_1 \to h\tilde{G}$	$\Lambda \cong 105$ TeV, $m_{\tilde{g}/\tilde{q}} \sim 1.5$ TeV, $\geq 3b$-jets + $E_{\text{T}}^{\text{miss}}$	$\Lambda \cong 140$ TeV $m_{\tilde{g}/\tilde{q}} \sim 2.0$ TeV, $\geq 2b$-jets + $E_{\text{T}}^{\text{miss}}$
E	$\tilde{Z}_1 \sim \tilde{h}$ $\tilde{Z}_1 \to Z\tilde{G}$	$\Lambda \cong 120$ TeV, $m_{\tilde{g}/\tilde{q}} \sim 1.3$ TeV, $\gamma\gamma + E_{\text{T}}^{\text{miss}}$	$\Lambda \cong 140$ TeV $m_{\tilde{g}/\tilde{q}} \sim 2.0$ TeV, $1l + E_{\text{T}}^{\text{miss}}$ Increase to 2.2 TeV via $Z\gamma + E_{\text{T}}^{\text{miss}}$ if excellent jet-γ rejection is available.
Reach in mSUGRA		$\tilde{m}_{\tilde{g}} \sim 0.35 - 0.4$ TeV $E_{\text{T}}^{\text{miss}}$	~ 1.6 TeV ($m_{\tilde{q}} \gg m_{\tilde{g}}$) $\ell + E_{\text{T}}^{\text{miss}}$ ~ 2.2 TeV ($m_{\tilde{q}} \sim m_{\tilde{g}}$) $\ell + E_{\text{T}}^{\text{miss}}$
Reach in mAMSB			~ 1.4 TeV ($m_{\tilde{q}} \gg m_{\tilde{g}}$) $E_{\text{T}}^{\text{miss}}$ ~ 2 TeV ($m_{\tilde{q}} \sim m_{\tilde{g}}$) $\ell^+\ell^- + E_{\text{T}}^{\text{miss}}$

https://doi.org/10.1017/9781009289801.016 Published online by Cambridge University Press

- The first concerns the reach of these machines for the different sparticles. The LHC is a broad band machine, where everything possible will be produced, though cross sections for the production of various sparticles will be very different. At LCs, all sparticles with non-vanishing $SU(2)_L \times U(1)_Y$ quantum numbers will be produced with comparable cross sections, and the reach will essentially be determined by the mass of the lightest visible sparticle. While it would be best to have a program of SUSY searches that is as model-independent as possible, it is also interesting to map out the reach of supercollider experiments for various SUSY models discussed in Chapter 11, and examine this in light of other constraints on the model parameter space.
- The second issue concerns how we would proceed if new physics is indeed discovered at the LHC. As discussed above, we would need to establish that the new physics is indeed softly broken supersymmetry. In this connection, we would embark upon a program of precision measurements of sparticle masses and other properties to unravel the mechanism by which sparticles obtain their masses, and ultimately determine the underlying physics and its associated parameters. We will postpone our discussion of this to the next section, while initially focussing upon the question of the SUSY reach.

15.4.1 Reach of the CERN LHC

We have seen that, in order to obtain an accurate representation of SUSY events for sparticles in the range of masses accessible at the LHC, it is essential to incorporate cascade decays. This is difficult to do within the MSSM because of the large number of free parameters. Instead, we use the various models introduced in Chapter 11 as a guide to our projections for the reach of the LHC. The other advantage of this procedure is that, because a large number of sparticles are expected to be simultaneously produced, contributions from all sparticle reactions to any particular event topology can be included in our exploration of the reach in that topology.

mSUGRA model

As we saw in Chapter 12, $\tilde{g}\tilde{g}$, $\tilde{g}\tilde{q}$, and $\tilde{q}\tilde{q}$ production processes are expected to be the dominant sparticle production mechanisms at the LHC. The cascade decay signatures will generally be very complex and give rise to events with jets, isolated leptons, and possibly isolated photons or Z^0 bosons (re-constructed via their leptonic decays) together with E_T^{miss}. Jets from primary decay of the squark or gluino can be very hard, reflecting the parent sparticle mass. Leptons (as well as other jets) that originate further down the cascade chain are typically softer than the primary jets in these events.

https://doi.org/10.1017/9781009289801.016 Published online by Cambridge University Press

The reach of the CERN LHC in the mSUGRA model has been evaluated by several groups.[10] The event topologies can be classified as before by the number of identified isolated leptons in the events:

1. $E_{\rm T}^{\rm miss}$ channel: an inclusive channel requiring large $E_{\rm T}^{\rm miss}$ plus ≥ 2 jets plus any number of identified leptons,
2. 0ℓ channel: a subset of the $E_{\rm T}^{\rm miss}$ channel which in addition vetoes any isolated leptons,
3. 1ℓ channel: a subset of $E_{\rm T}^{\rm miss}$ containing a single isolated lepton,
4. OS channel: a subset of $E_{\rm T}^{\rm miss}$ containing two opposite-sign isolated leptons,
5. SS channel: a subset of $E_{\rm T}^{\rm miss}$ containing two same-sign isolated leptons,
6. 3ℓ channel: a subset of $E_{\rm T}^{\rm miss}$ containing three isolated leptons.

Larger lepton multiplicities can also occur, but at lower rates.

The SUSY reach of the LHC within the framework of the mSUGRA model is illustrated in Fig. 15.6 in the $m_0 - m_{1/2}$ plane, with $A_0 = 0$, $\tan\beta = 30$, and $\mu > 0$. As before, the dark (light) shaded regions are excluded by theoretical (experimental) constraints. Also shown are contours where $m_{\tilde{g}}$ or $m_{\tilde{u}_{\rm L}}$ is 2 TeV. In the figure, many sets of cuts were examined. For each point in the plane, the cuts were chosen to optimize the signal relative to the background. The region below the various curves is where LHC experiments should be able to see a signal at the 5σ level with a minimum of ten signal events in the event topology shown on the contour, assuming an integrated luminosity of 100 fb^{-1}. The cumulative reach in all the channels is shown by the solid contour labelled $E_{\rm T}^{\rm miss}$. We see that LHC experiments should be able to explore $m_{1/2}$ values up to 1400 (700) GeV for small (very large) values of m_0, corresponding to $m_{\tilde{g}} = 3(1.8)$ TeV. Moreover, if $m_{\tilde{g}} \lesssim 1.5$–2 TeV, there should be an observable signal in several channels if the observed signal is to be attributed to SUSY as realized in this framework. The reach results are qualitatively similar for other values of $\tan\beta$ or the opposite sign of μ.

It is also worth mentioning that the trilepton signal from $\widetilde{W}_1\widetilde{Z}_2$ production may also be observable above backgrounds at the LHC provided $m_{1/2}$ is not too large.[11] For large values of $m_{1/2}$ the two-body decay $\widetilde{Z}_2 \to \widetilde{Z}_1 h$ or $\widetilde{Z}_2 \to \widetilde{Z}_1 Z$ becomes accessible and quickly dominates the $\widetilde{Z}_2$ decay rate unless sleptons are also light so that $\widetilde{Z}_2 \to \tilde{\ell}_{\rm L,R}\ell$ decays are also accessible. Direct production of sleptons leads to an observable signal (above W^+W^- and $t\bar{t}$ backgrounds) in the $\ell^+\ell^- + E_{\rm T}^{\rm miss}$ channel if sleptons are lighter than 250 GeV (300 GeV if soft jets can be efficiently vetoed).[12]

[10] H. Baer *et al.*, *Phys. Rev.* **D52**, 2746 (1995), *Phys. Rev.* **D53**, 6241 (1996) and *Phys. Rev.* **D59**, 055014 (1999); S. Abdullin and F. Charles, *Nucl. Phys.* **B547**, 60 (1999); S. Abdullin *et al.* (CMS Collaboration), hep-ph/9806366 (1998); B. Allanach *et al.*, *JHEP* **08**, 017 (2000); H. Baer *et al.*, *JHEP* **0306**, 054 (2003).

[11] H. Baer *et al.*, *Phys. Rev.* **D50**, 4508 (1994); I. Iashvili and A. Kharchilava, *Nucl. Phys.* **B526**, 153 (1998).

[12] H. Baer, C. H. Chen, F. Paige and X. Tata, *Phys. Rev.* **D49**, 3283 (1994); D. Denegri, W. Majerotto and L. Rurua, *Phys. Rev.* **D58**, 095010 (1998).

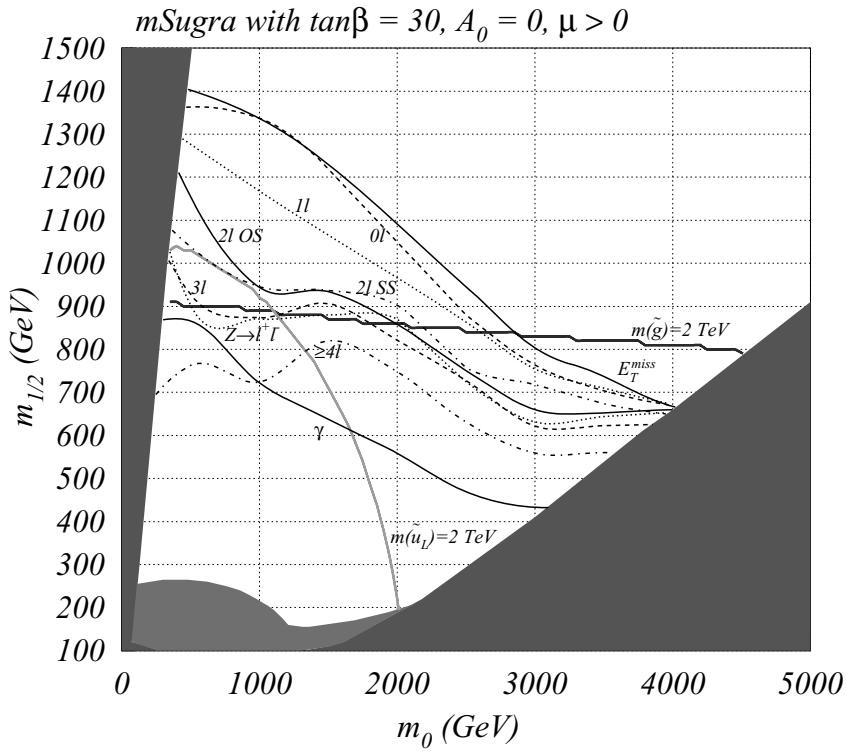

Figure 15.6 The 5σ reach of the CERN LHC in the $m_0 - m_{1/2}$ plane of the mSUGRA model for an integrated luminosity of 100 fb^{-1}. The shaded regions are excluded by theoretical and experimental constraints discussed in the text. Below each of the labelled contours, there should be an observable signal at the LHC in the corresponding channel. Reprinted from H. Baer, C. Balázs, A. Belyaev, T. Krupovnickas and X. Tata, *JHEP* **06**, 054 (2003).

In Fig. 15.7, we illustrate the interplay between various measurements within a constrained framework, using mSUGRA with the same parameters as in the previous figure as an example. The dark shaded regions are excluded by theoretical considerations as shown on the figure, while the light shaded region (labelled LEP2) is excluded by the chargino constraint from LEP2 experiments. Below the unlabeled contour starting around $m_{1/2} = 270$ GeV, $m_h < 114$ GeV. The jagged circular contours labeled 2 and 3 are contours above which $B(B \to X_s\gamma) > 2(3) \times 10^{-4}$, the region favored by experiment. The slanted lines labeled 1, 2, 5, . . . 40 are contours of the SUSY contribution to a_μ, the anomalous magnetic moment of the muon. Between the dotted/dashed contours along the boundaries of the theoretically excluded regions, the neutralino relic density agrees with its determination by the WMAP collaboration, while the corresponding solid line is the contour of $\Omega_{\tilde{Z}_1} h^2 = 1$. The

https://doi.org/10.1017/9781009289801.016 Published online by Cambridge University Press

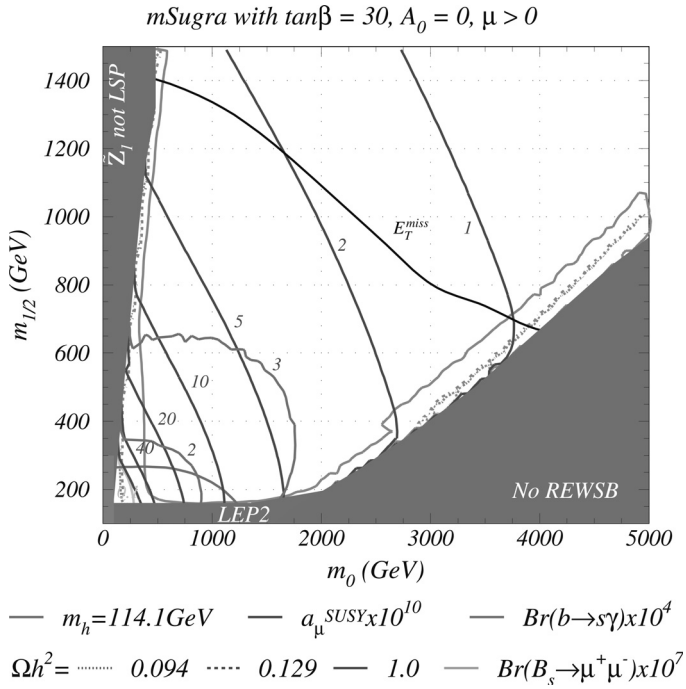

Figure 15.7 The SUSY reach of the CERN LHC within the mSUGRA model, together with contours of $B(B \to X_s\gamma)$, $a_\mu^{\rm SUSY}$, and the neutralino relic density. In the lighter-shaded lower part of the theoretically excluded wedge region on the left, the stau mass squared is negative. Reprinted from H. Baer, C. Balázs, A. Belyaev, T. Krupovnickas and X. Tata, *JHEP* **06**, 054 (2003).

WMAP experiment requires us to lie in the narrow slivers between the theoretically excluded region, and the dashed line, where neutralinos can annihilate efficiently either due to co-annihilation with staus (left side WMAP region) or due to a significant higgsino admixture of the $\widetilde{Z}_1$ in the HB/FP region at large m_0. The contour labeled $E_{\rm T}^{\rm miss}$ shows the cumulative reach of LHC experiments as we have just discussed. We see that essentially the entire stau co-annihilation region can be probed at the LHC. The HB/FP region, however, continues indefinitely, and new strategies may be needed to extend the reach in this region.[13] An unambiguous observation of a deviation from SM expectation of the muon anomalous magnetic moment or of non-standard flavor-violating decays of B or B_s mesons will preclude nature from being in the part of the HB/FP region that is beyond the reach of the LHC. If such a deviation is to be attributed to the mSUGRA realization of SUSY, then there must be observable signals at the LHC.

[13] For very large values of tan β there is another WMAP allowed region where neutralinos can annihilate efficiently via H and A exchange in the s-channel. Again, LHC experiments can probe most, but not all, of this region.

https://doi.org/10.1017/9781009289801.016 Published online by Cambridge University Press

GMSB models

The SUSY reach at the LHC within the GMSB framework has also been computed, using the same model lines as for the Tevatron. The results are summarized in Table 15.2 where the channel via which the reach is obtained is also shown assuming an integrated luminosity of 10 fb^{-1}.[14] We see that the reach is *at least* as good as in the mSUGRA framework, but that for model line **A** (**C**) the presence of additional photons (leptons) serves to reduce the background resulting in a significantly increased reach. We mention that for model line **C**, LHC experiments will be able to search for direct production of $\tilde{\ell}_R$ pairs if $m_{\tilde{\ell}_R} \lesssim 280$ GeV.

mAMSB model

In the mAMSB model, the LSP is the $\widetilde{Z}_1$, but it is wino-like, and typically just $\sim$ 160–200 MeV lighter than the chargino. Charginos which are produced directly or in cascade decays decay to a soft charged pion plus the escaping $\widetilde{Z}_1$ so that it is nearly invisible in the experimental apparatus. Although these charginos typically fly just a few centimeters before decaying, some may leave a terminating track, or a track with a kink in the apparatus. Whether these distinctive signatures of SUSY events (which would have to be triggered by some other means) will be observable depends on details of the detector.[15]

It is interesting to explore the LHC reach using the general search strategies for SUSY. It is expedient to present our results for the reach via various multijet + multilepton + E_T^{miss} channels in the $m_0 - m_{3/2}$ plane. Sample results are shown in Fig. 15.8 for $\tan\beta = 35$ and $\mu > 0$. In this framework, $\tilde{q}_R$ mainly decays to the bino-like $\widetilde{Z}_2$ (if this decay is kinematically allowed); the subsequent $\widetilde{Z}_2$ decays give rise to isolated leptons. In contrast, $\tilde{q}_L$ decays to $\widetilde{Z}_1$ or $\widetilde{W}_1$, and gives jets + E_T^{miss}. The situation with cascades is just the opposite of models with gaugino mass unification where it is $\tilde{q}_L$ that cascade decays while $\tilde{q}_R$ mostly decays directly to the LSP. In the low m_0 large $m_{3/2}$ region, $\tilde{g} \to \tilde{t}_1 t$, which gives rise to leptons from top and stop decay. The best reach is in the OS dilepton channel where values of $m_{\tilde{g}} \gtrsim 2$ TeV can be probed in 10 fb^{-1} of data. At high m_0, $\tilde{g} \to q\bar{q}\widetilde{Z}_1$ or $q\bar{q}'\widetilde{W}_1$, and the best reach

[14] H. Baer *et al.*, *Phys. Rev.* **D62**, 095007 (2000).

[15] In a typical collider experiment, it is not possible to record every event because the collision rate is too large for the data acquisition system to handle. Most of these events are small angle elastic or quasi-elastic collisions and not of any interest. In order to ensure that potentially interesting events are all recorded without the data acquisition system being completely swamped, experimentalists set up loose criteria that events must satisfy in order to be recorded. These criteria, referred to as trigger requirements, could for instance require the presence of high E_T jets, isolated hard leptons or photons, or large amounts of E_T^{miss} to reduce event rates to manageable levels. The challenge is to arrive at a decision as to whether or not to record an event in a short time, since collisions are continually occuring in the apparatus. The development of triggers is a complicated but essential issue for all collider experiments, but especially so at the hadron colliders where the total cross section is very large.

https://doi.org/10.1017/9781009289801.016 Published online by Cambridge University Press

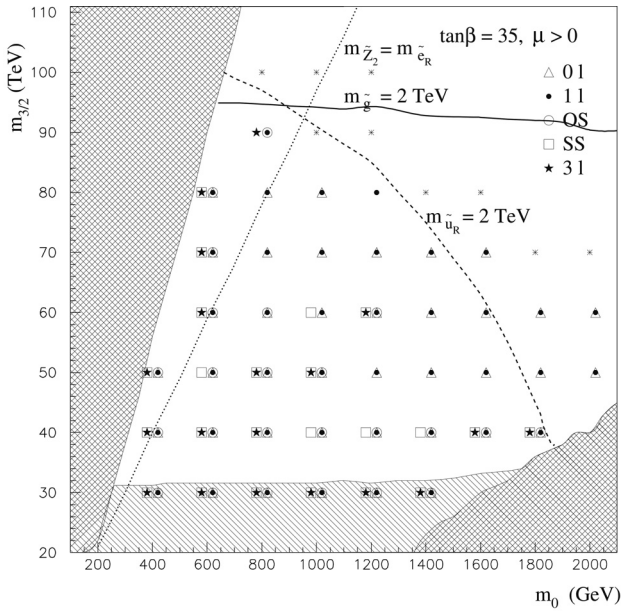

Figure 15.8 The reach of the CERN LHC for mAMSB for $\tan\beta = 35$, $\mu > 0$, and 10 fb^{-1} of integrated luminosity. Reprinted with permission from H. Baer, J. K. Mizukoshi and X. Tata, *Phys. Lett.* **B488**, 367 (2000).

occurs in the 0ℓ + jets + $E_{\rm T}^{\rm miss}$ channel, where values of $m_{\tilde{g}} \sim 1350$ GeV may be probed with just 10 fb^{-1} of data.

LHC reach for SUSY Higgs bosons

The experiments at LEP2 have already placed stringent bounds on Higgs boson masses in the MSSM, and Tevatron experiments may well find evidence for the light scalar h before LHC turns on. Nevertheless, it will be an important task for the CMS and ATLAS experiments to establish the Higgs boson content of the MSSM, and to determine as much as possible about their properties.

The Higgs boson search is complicated and will have to be performed using many channels. For h produced in the s-channel via gg fusion, SM backgrounds preclude the possibility of seeing a signal from its dominant decays $h \to b\bar{b}$ or $h \to \tau^+\tau^-$; the rare decay

$$pp \to hX;\ h \to \gamma\gamma$$

appears to be viable, but will require several years of LHC operation to establish a signal. Excellent electromagnetic calorimetry is essential to see the $h \to \gamma\gamma$ mass bump above the enormous $q\bar{q}, gg \to \gamma\gamma$ continuum background. This will yield an accurate determination of m_h. If squarks and gluinos are not too heavy, the SUSY

https://doi.org/10.1017/9781009289801.016 Published online by Cambridge University Press

event sample at the LHC may also include a small number of events with clearly identified $h \to \gamma\gamma$ decays, thus establishing h production in SUSY cascade decay events.

For moderate to large values of $\tan\beta$, s-channel H and A production may be visible via the decay modes $H, A \to \mu\bar{\mu}, \tau\bar{\tau}$. For smaller values of $\tan\beta$, $H, A \to t\bar{t}$, $H \to ZZ^{(*)} \to 4\ell$, $A \to Zh \to \ell^+\ell^- b\bar{b}$, and $H \to hh \to b\bar{b}\gamma\gamma$ may also be observable.

Higgs bosons can also be produced at large rates in association with heavy quarks. The reactions

$$pp \to t\bar{t}h,\ b\bar{b}h,\ b\bar{b}A,\ \text{and}\ b\bar{b}H$$

may all be visible, where the Higgs bosons generally decay to $b\bar{b}$ or $\gamma\gamma$ final states. Higgs bosons can also be produced in association with vector bosons, and their detection via $pp \to Wh \to \ell\nu_\ell\gamma\gamma$ is possible in some part of the plane. The charged Higgs boson may be visible as well at LHC if it can be produced in $t \to bH^+$ decays.

The results of many detailed studies of the capability of LHC experiments are summarized in Fig. 15.9, where it is assumed that Higgs bosons cannot decay to sparticles. It appears that over essentially the entire m_A $-$ $\tan\beta$ parameter space, LHC experiments should be able to discover at least one Higgs boson. The search for SUSY Higgs bosons in many of these channels is difficult, and very large integrated luminosities and excellent detector performance will be necessary. Even so, a small region around $m_A \sim 150$ GeV and $\tan\beta \sim 5-10$ seems difficult, and requires further improvement in the resolution of $b\bar{b}$ dijet invariant masses. Fortunately, Higgs bosons in this "hole" should be easy to study at a 500 GeV e^+e^- collider. It is also gratifying to see that over significant portions of the plane there is an observable signal from more than one Higgs boson: this may serve to distinguish the MSSM Higgs sector from that of the SM.

If SUSY particles are accessible in LHC experiments, it is quite possible that the lightest Higgs scalar h will be discovered first in the SUSY particle event sample as a $h \to b\bar{b}$ mass bump. The parameter space "hole" mentioned above might be explored in this way. Moreover, if some sparticles are light, then Higgs bosons will have significant branching fractions for decays to SUSY particles. Higgs boson decays to SUSY particles will in general diminish the SM decay modes, and may make the search modes listed in Fig. 15.9 more difficult. Decays of neutral Higgs bosons to $\widetilde{Z}_1\widetilde{Z}_1$ states would yield "invisible" Higgs bosons. It is also possible that Higgs boson decays to SUSY particles will open up new, sometimes spectacular, search channels. As an example, H may decay via $H \to \widetilde{Z}_2\widetilde{Z}_2 \to \ell\bar{\ell}\ell'\bar{\ell}' + E_{\mathrm{T}}^{\mathrm{miss}}$. The 4ℓ final state will have an invariant mass $\leq (m_H - 2m_{\widetilde{Z}_1})$, and can be visible over restricted regions of MSSM parameter space.

https://doi.org/10.1017/9781009289801.016 Published online by Cambridge University Press

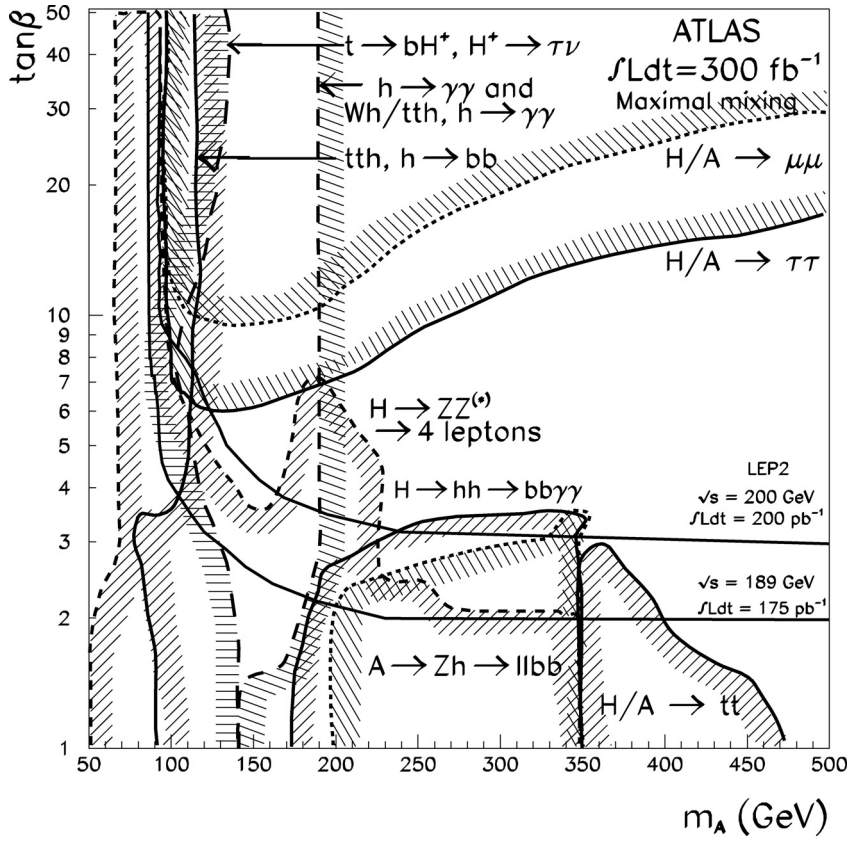

Figure 15.9 The reach of the CERN LHC for SUSY Higgs bosons in the case of heavy sparticles. The signal is detectable on the side of the contour where the shading appears. This figure is reprinted from the ATLAS Technical Design Report.

15.4.2 SUSY reach of e^+e^- colliders

Since $m_h \lesssim 130$–135 GeV in the MSSM, an e^+e^- collider operating at $\sqrt{s} \geq 500$ GeV is sure to access the lightest SUSY Higgs scalar h. If the couplings of h are nearly those of the SM Higgs boson (as it is over much of mSUGRA parameter space) the cross section for the "Higgstrahlung" process

$$e^+e^- \to Zh \tag{15.8a}$$

is large and offers a good channel for h detection above SM backgrounds. The ZZh coupling can become rather small if m_A is light; in this case, the ZhA coupling is necessarily large so that h would be produced via

$$e^+e^- \to Ah, \tag{15.8b}$$

https://doi.org/10.1017/9781009289801.016 Published online by Cambridge University Press

and would also not escape detection. Indeed, not seeing any signal for h would exclude the MSSM as the low energy theory valid up to the GUT scale. Over parts of the parameter space, H and $H^{\pm}$ may also be accessible via the processes

$$e^+e^- \to ZH, \text{ or } H^+H^-. \tag{15.8c}$$

Unequivocal identification of Higgs bosons produced via either (15.8b) or (15.8c) will signal a non-minimal Higgs boson sector, though not necessarily supersymmetry.

The reach of a LC for visibly decaying superpartners is limited mainly by the beam energy. For the mSUGRA model, candidates for the lightest of these visible supersymmetric particles (LVSP) include the $\widetilde{W}_1$ or $\widetilde{Z}_2$, one of the sleptons (usually the lightest stau $\tilde{\tau}_1$) and sometimes the lightest of the third generation squarks. Apart from the $\widetilde{Z}_2$, whose production can be strongly suppressed, the other LVSP candidates are expected to be produced with cross sections (aside from kinematic suppression) typical of electroweak processes: $\sim(10-100)$ fb$/\sqrt{s}$, with $\sqrt{s}$ in TeV units. Since sparticle production is readily distinguishable from SM processes, it should be possible to detect these at LCs with an integrated luminosity of several tens of fb^{-1}.

If $\sqrt{s} > 2m_{\widetilde{W}_1}$, then chargino pair production ought to be visible above SM backgrounds. The background would consist mainly of W^+W^- production. In $\ell + 2$-jets or 4-jet events, this background can be rejected by requiring cuts on missing mass $\not{m}$ defined as $\not{m} = \sqrt{\not{E}^2 - \not{p}^2}$. For SUSY, $\not{m} > 2m_{\widetilde{Z}_1}$, while for WW background, $\not{m} = 0$ for perfect energy and momentum measurements. Another discriminator in $\ell + 2$-jet events is the distribution in E_{jj}, the energy of all jets: for WW production, $E_{jj} = E_W = \sqrt{s}/2$, while for $\widetilde{W}_1^+\widetilde{W}_1^-$ production with three-body $\widetilde{W}_1^{\pm}$ decays, there is a continuum of values. In the HB/FP region where $|\mu| \lesssim |M_2|$, the chargino and neutralino become close in mass and the visible energy is small. In this case, specialized cuts are needed to select the signal over the various SM backgrounds that, in this case, include $2 \to 3$ and $2 \to 4$ processes.[16]

If instead $\tilde{\tau}_1$ is the LVSP, or several sleptons are co-LVSPs, then the signature is

$$e^+e^- \to \tilde{\ell}^+\tilde{\ell}^- \to \ell^+\ell^- + \not{E}. \tag{15.9}$$

The presence of acoplanar OS dilepton pairs in excess of expectations from WW and ZZ production would signal the production of sleptons. The scalar pair production reactions are suppressed by the usual β^3 factor near threshold. In addition, in mSUGRA it is possible to have nearly degenerate $\tilde{\ell}$ and $\widetilde{Z}_1$, in which case the visible energy from slepton decay will be small, and detection efficiency will be reduced.

[16] H. Baer *et al.*, *JHEP* **02**, 007 (2004).

https://doi.org/10.1017/9781009289801.016 Published online by Cambridge University Press

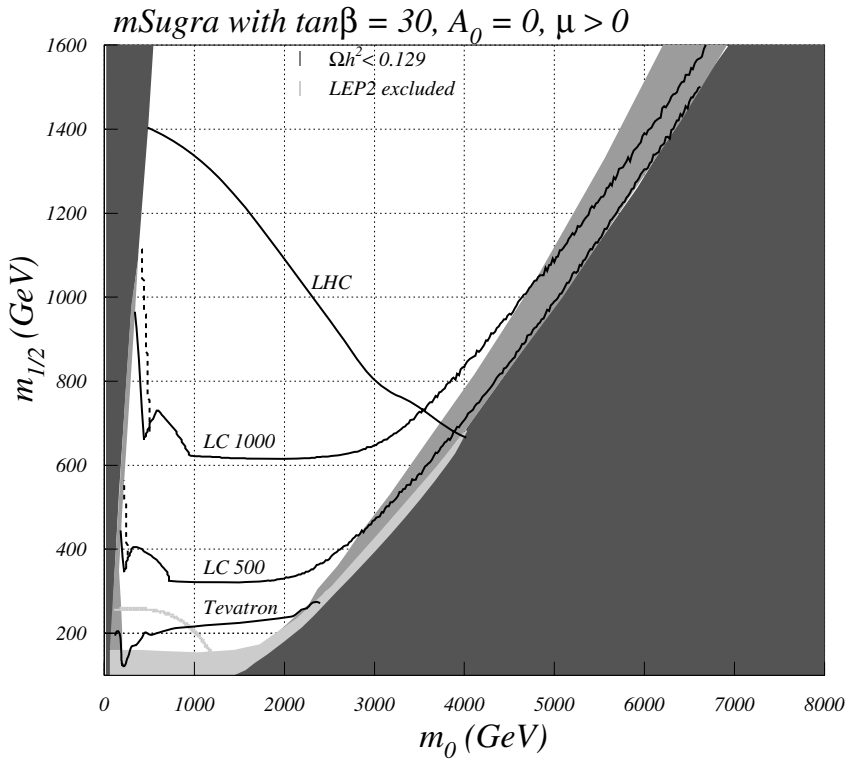

Figure 15.10 The SUSY reach of an e^+e^- LC with $\sqrt{s} = 500$ and 1000 GeV within the mSUGRA model with $A_0 = 0$, $\tan\beta = 30$, and $\mu > 0$, assuming an integrated luminosity of 100 fb^{-1}. The darkest (lightest) shaded regions are excluded by theoretical (experimental) constraints. Below the gray arc in the bottom left corner, $m_h < 114$ GeV. The medium gray shaded regions of the plane run along the boundary of the theoretically excluded wedge at small values of m_0, and in the HB/FP region close to the boundary of the theoretically excluded region on the right: in these regions, the predicted neutralino relic density is consistent with the results of the WMAP collaboration. Finally, contours showing the reaches of Fermilab Tevatron upgrades assuming an integrated luminosity of 25 fb^{-1}, and the CERN LHC with 100 fb^{-1} of integrated luminosity, are also shown for comparison. Reprinted from H. Baer, A. Belyaev, T. Krupovnickas and X. Tata, *JHEP* **02**, 007 (2004).

Our projection for the reach of an e^+e^- LC with $\sqrt{s} = 500$ or 1000 GeV is shown in Fig. 15.10, assuming an integrated luminosity of 100 fb^{-1}. We work within the mSUGRA framework and, as in Fig. 15.6, show the reach in the $m_0 - m_{1/2}$ plane, and fix $A_0 = 0, \tan\beta = 30$ and $\mu > 0$. The darkest region is excluded by theoretical constraints that we have already discussed, while the medium gray region at low values of $m_{1/2}$ is excluded by experimental constraints from LEP experiments. The contours labeled "LC 500" and "LC 1000" are the envelope of the regions below which experiments at a LC operating at $\sqrt{s} = 500$ or 1000 GeV should be able

https://doi.org/10.1017/9781009289801.016 Published online by Cambridge University Press

to detect a signal for sparticle production above SM backgrounds. These contours are a composite of the contours below which slepton pair production (the falling part of the contour at small m_0) or chargino pair production (the flat portion of the contour, rising to large values of $m_{1/2}$ close to the excluded region on the right) should be detectable. The kinematic reach of a LC for $\tilde{\tau}_1\bar{\tilde{\tau}}_1$ pairs is denoted by the dashed contours. For very large values of m_0 in the HB/FP region, the chargino is light and higgsino-like and becomes increasingly mass degenerate with $\widetilde{Z}_1$. In this case, the visible energy from $\widetilde{W}_1^+\widetilde{W}_1^-$ production followed by $\widetilde{W}_1 \to \widetilde{Z}_1 f \bar{f}'$ decay becomes very small, and the signal must be extracted using a specialized analysis. Finally, the bulge in the contours near $m_0 \sim 300$–1000 GeV shows the additional region where the signal from

$$e^+e^- \to \widetilde{Z}_1 + \widetilde{Z}_2 \to \widetilde{Z}_1 + \widetilde{Z}_1 h \to \widetilde{Z}_1 + \widetilde{Z}_1 b\bar{b}$$

production is observable. Also shown for comparison are contours corresponding to the reach of Tevatron upgrades and the reach of the LHC, assuming an integrated luminosity of 100 fb^{-1}, taken from Fig. 15.6. The lightest gray regions are where the cosmological neutralino relic density $\Omega_{\widetilde{Z}_1}h^2 < 0.129$ as required by its determination by the WMAP collaboration. As mentioned in Section 15.4.1, the HB/FP region is one of the regions of the mSUGRA parameter space consistent with the WMAP relic density determination. We see from Fig. 15.10 that experiments at linear colliders will be able to probe beyond the LHC reach in this favored part of mSUGRA parameter space.

In GMSB models with a low SUSY breaking scale, the gravitino is the LSP. Generally speaking, the presence of additional photons or leptons from NLSP decays should make the detection of any sparticle signal easier. Moreover, if $\widetilde{Z}_1$ is the NLSP, then

$$e^+e^- \to \widetilde{Z}_1\widetilde{Z}_1 \to \gamma\gamma + E_{\rm T}^{\rm miss} \tag{15.10}$$

should also be observable as long as $\widetilde{Z}_1$ decays inside the detector, though in the case of delayed decays this would require the identification of photons that are very displaced from the primary vertex. As long as this is possible, the reach should be close to the kinematic limit since t-channel neutralino production is not particularly suppressed. If instead a slepton is the NLSP, and decays promptly via $\tilde{\ell} \to \ell\tilde{G}$, then

$$e^+e^- \to \tilde{\ell}^+\tilde{\ell}^- \to \ell^+\ell^- + E_{\rm T}^{\rm miss} \tag{15.11}$$

should have a similar reach as for the case where the slepton is the LVSP in the mSUGRA framework. If the slepton decay is delayed, the reaction can still be detected via searches for tracks with kinks or from searches for quasi-stable slow moving massive exotics that may reveal themselves through highly ionizing tracks.

https://doi.org/10.1017/9781009289801.016 Published online by Cambridge University Press

In the AMSB model, the $SU(2)$ gaugino-like chargino is the LVSP. However, signals from chargino pair production will be difficult to detect because the tiny $\widetilde{W}_1 - \widetilde{Z}_1$ mass gap implies that the visible decay products of the chargino carry very little energy. In this case, the process $e^+e^- \to \widetilde{W}_1^+ \widetilde{W}_1^- \gamma$ offers the best hope for detection. If $\widetilde{W}_1$ dominantly decays via $\widetilde{W}_1 \to \widetilde{Z}_1 \pi$, and the pion (whose energy is several hundred MeV) is detectable, its presence serves to reduce background from $e^+e^- \to \gamma \nu \bar{\nu}$ events in the SM. The background from $e^+e^- \to e^+e^- \gamma$ events can be controlled as long as there is some instrumentation in the beam direction.

15.5 Beyond SUSY discovery

If new physics is discovered at the LHC in one or more of the several channels that we have discussed above, it will mark the start of the program to establish that it is softly broken SUSY (or something else) and to determine the mechanism by which SUSY is broken. The discovery of several superpartners (with expected spins and gauge quantum numbers), either via their direct production or more likely via a reconstruction of cascade decay chains at the LHC, will make a strong case for SUSY. That the new physics is SUSY can be conclusively established by experiments showing that couplings of superpartners are related to those of their SM partners: this should be possible via precision measurements that are possible at LCs. The determination of the sparticle masses as well as cross sections and branching ratios (these provide information about their couplings) will be the first step to elucidating the mechanism of SUSY breaking, since these will provide information about the underlying SSB parameters. Such measurements, which should be possible at the LHC as well as LCs, will also serve to rule in or rule out various models that we have considered in Chapter 11, and in the former case also provide information about the underlying parameters.

15.5.1 Precision SUSY measurements at the LHC

Once a sufficient number of SUSY scattering events is accumulated, the task will turn to scrutinization of the events to try to make precision measurements of sparticle masses, branching fractions, spin and other quantum numbers, marking the start of sparticle spectroscopy. As discussed at the start of Section 12.2, the environment of hadron collisions poses formidable difficulties for precision measurements. Nevertheless, experience at the CERN S$p\bar{p}$S and Fermilab Tevatron, where M_W has been determined very precisely in spite of the undetected neutrino in these events, has taught us that precision measurements are indeed possible. We should, therefore, maintain a positive outlook, and critically examine how well SUSY particle properties can be determined at the LHC.

https://doi.org/10.1017/9781009289801.016 Published online by Cambridge University Press

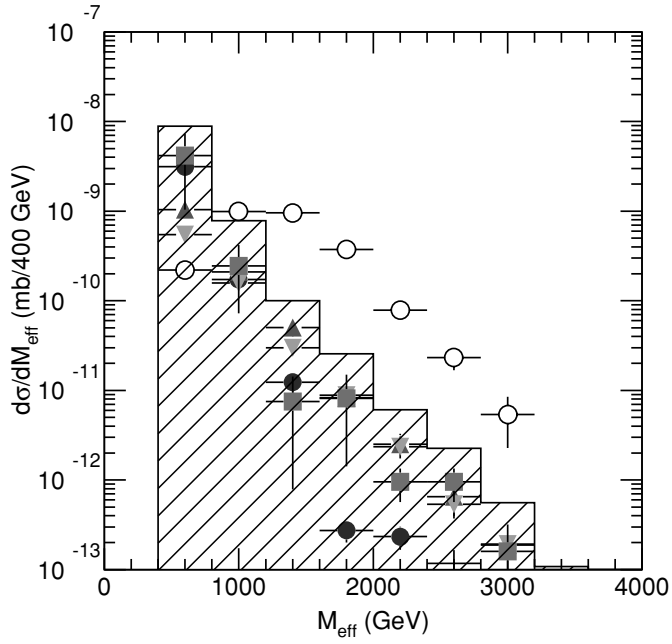

Figure 15.11 Distribution in $M_{\rm eff}$ for SUSY events in the mSUGRA model with $m_0 = 100$ GeV, $m_{1/2} = 300$ GeV, $\tan\beta = 2.1$, $A_0 = 300$ GeV, and $\mu > 0$ (open circles) and for the SM background (histogram) from $t\bar{t}$ production (solid circles), W + jets (upright triangles), Z + jets (upside down triangles), and QCD jets (squares). Reprinted from the ATLAS Technical Design Report.

Since gluino and squark pair production cross sections are expected to be the dominant SUSY cross sections at the LHC, a first estimate of the SUSY particle mass scale will be obtained from the magnitudes of the momenta of jets and $E_{\rm T}^{\rm miss}$ in these events: heavier sparticles lead to harder jets and $E_{\rm T}^{\rm miss}$. In Fig. 15.11, we show the distribution of the effective mass

$$M_{\rm eff} = E_{\rm T}^{\rm miss} + E_{\rm T}(\text{jet 1}) + E_{\rm T}(\text{jet 2}) + E_{\rm T}(\text{jet 3}) + E_{\rm T}(\text{jet 4}) \qquad (15.12)$$

for SUSY events in the mSUGRA model with $m_0 = 100$ GeV, $m_{1/2} = 300$ GeV, $\tan\beta = 2.1$, $A_0 = 300$ GeV, and $\mu > 0$, for which $m_{\tilde{g}} \simeq 767$ GeV and $m_{\tilde{q}} \simeq 680$ GeV.[17] Also shown is the same distribution for SM events. Clearly, for large values of $M_{\rm eff}$, the signal emerges from the falling background distribution. It has been shown that the peak of the SUSY $M_{\rm eff}$ distribution correlates surprisingly well with $M_{\rm SUSY} = \min(m_{\tilde{g}}, m_{\tilde{q}})$, and yields a good first guess as to the SUSY particle mass scale.

[17] It is unimportant for the present discussion that this model, which was examined for ATLAS feasibility studies, is now excluded both by the bound on m_h as well as by WMAP constraints.

https://doi.org/10.1017/9781009289801.016 Published online by Cambridge University Press

Detailed determination of sparticle masses is complicated by the fact that every event has *two* undetected particles. Even so, as discussed below, the determination of kinematic "mass edges" constrains particular combinations of masses in SUSY events. If enough such kinematic "end points" can be measured, it may be possible to determine individual sparticle masses. Frequently though, it may be possible to directly determine only mass differences.

The simplest example of a measurable mass edge in SUSY events is the upper limit on the invariant mass of dileptons from $\widetilde{Z}_2 \to \ell\bar{\ell}\widetilde{Z}_1$ decays:

$$m(\ell\bar{\ell}) \leq m_{\widetilde{Z}_2} - m_{\widetilde{Z}_1} \tag{15.13a}$$

regardless of whether the $\widetilde{Z}_2$ is produced directly or in cascade decays. Even allowing for experimental resolution, the end point of this distribution can be well determined as long as the leptonic branching fraction for $\widetilde{Z}_2$ decays is not strongly suppressed. The end point (15.13a) is attained when the two leptons recoil against one another with $\widetilde{Z}_1$ stationary in the rest frame of $\widetilde{Z}_2$. This end point is not kinematically accessible if $\widetilde{Z}_2 \to \tilde{\ell}\bar{\ell} \to \ell\widetilde{Z}_1\bar{\ell}$ with the intermediate slepton on its mass shell because kinematic constraints do not allow $\widetilde{Z}_1$ to be at rest. In this case, except for slepton width effects and tiny contributions from off-shell sleptons, the kinematic end point shifts to

$$m(\ell\bar{\ell}) < m_{\widetilde{Z}_2}\sqrt{1-\frac{m^2_{\tilde{\ell}}}{m^2_{\widetilde{Z}_2}}}\sqrt{1-\frac{m^2_{\widetilde{Z}_1}}{m^2_{\tilde{\ell}}}} \leq m_{\widetilde{Z}_2} - m_{\widetilde{Z}_1}. \tag{15.13b}$$

Once the overall SUSY mass scale is established using the $M_{\rm eff}$ variable, then attention can be focussed on reconstructing particular decay chains.[18] Although many studies have been performed to examine how this might be done, we use the mSUGRA model with parameters in Fig. 15.11 as an illustration of how one might proceed. The decay $\widetilde{Z}_2 \to \ell\bar{\ell}\widetilde{Z}_1$ just discussed serves as an important starting point. The distribution of opposite sign, same flavor dilepton masses in events with jets plus $E_{\rm T}^{\rm miss}$ events is shown in Fig. 15.12. Some care must be exercised in extracting information from this measured end point because one does not a priori know the decay pattern of $\widetilde{Z}_2$, though the large number of dileptons may hint at its decay via a real slepton. Indeed, we see a distinct mass edge above SM backgrounds and SUSY contamination close to its expected location, $m(\ell\bar{\ell})^{\rm exp} = 108.6$ GeV. The large event rate implies that this dilepton mass edge can be measured to a precision of well below a GeV.

[18] These studies were pioneered by I. Hinchliffe *et al.*, *Phys. Rev.* **D55**, 5520 (1997) and *Phys. Rev.* **D60**, 095002 (1999); H. Bachacou, I. Hinchliffe, and F. Paige, *Phys. Rev.* **D62**, 015009 (2000); Atlas Collaboration, *Atlas Physics and Detector Performance Technical Design Report*, LHCC 99-14/15.

https://doi.org/10.1017/9781009289801.016 Published online by Cambridge University Press

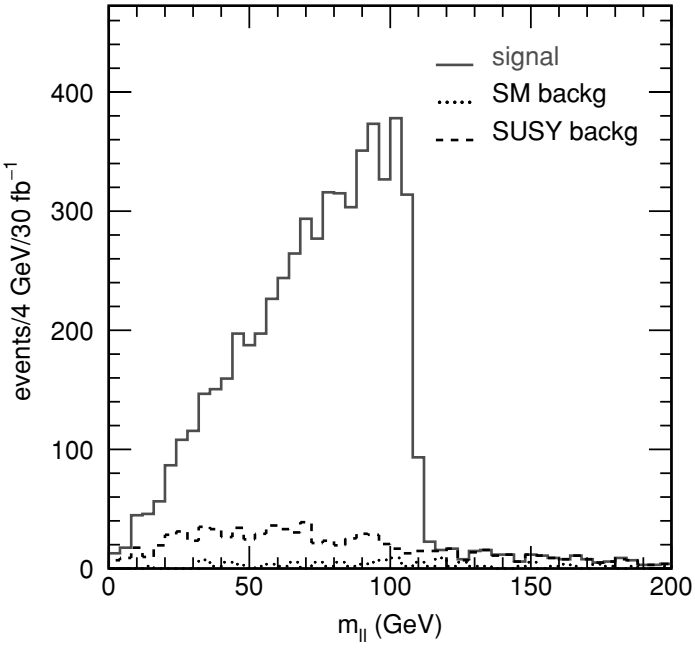

Figure 15.12 Distribution in $m(\ell\bar{\ell})$ for signal (solid) and SM (dots) and SUSY background (dashes) for the mSUGRA point with the same model parameters as in Fig. 15.11. Reprinted from the ATLAS Technical Design Report.

The next step in reconstructing the cascade decay

$$\tilde{q}_{\mathrm{L}} \to q\widetilde{Z}_2 \to q\tilde{\ell}^{\pm}\ell^{\mp} \to q\ell^{\pm}\ell^{\mp}\widetilde{Z}_1, \tag{15.14}$$

which has a large branching fraction, is to combine the dilepton invariant mass with one of the high p_{T} jets in the event. Typically there are two or more high p_{T} jets in each SUSY event. One may construct the $m(\ell\bar{\ell}q)$ invariant mass for each of the highest p_{T} jets, and plot the smaller of the two combinations. This distribution is shown in Fig. 15.13, which is plotted for the lepton combinations $e^+e^- + \mu^+\mu^- - \mathrm{e}^{\pm}\mu^{\mp}$ to statistically remove the contamination from squark decays to chargino pairs. Even for the assumed decay chain, the formula for the kinematic end point depends on the various masses (see exercise below), but an a-posteriori justification of any choice is possible if sparticle masses can be extracted from the data. For our choice of masses, assuming that the combination with the lower mass is the one from the decay of a single squark, we have

$$m(\ell\bar{\ell}q) < m_{\tilde{q}}\sqrt{1-\frac{m^2_{\widetilde{Z}_2}}{m^2_{\tilde{q}}}}\sqrt{1-\frac{m^2_{\widetilde{Z}_1}}{m^2_{\widetilde{Z}_2}}} = 552.4\ \mathrm{GeV}. \tag{15.15}$$

https://doi.org/10.1017/9781009289801.016 Published online by Cambridge University Press

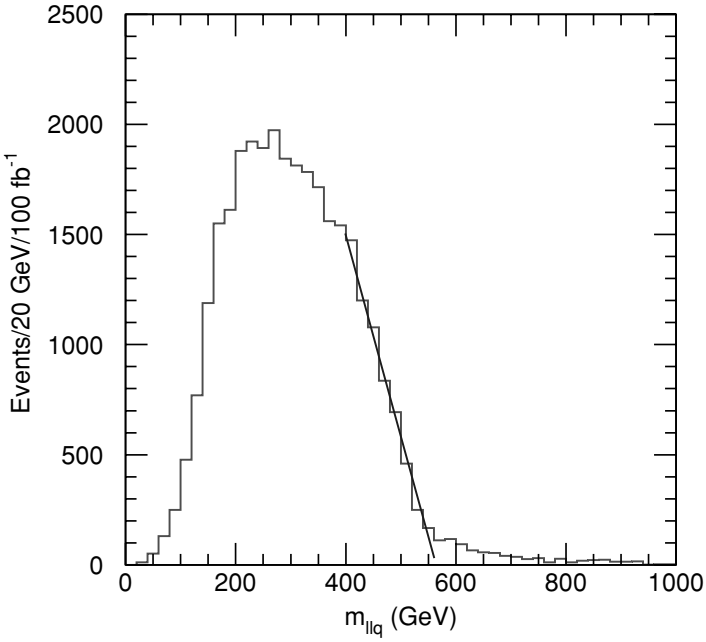

Figure 15.13 Distribution in $m(\ell\bar{\ell}q)$ for the smaller of the two $\ell^+\ell^-q$ invariant mass combinations for the mSUGRA model of the previous figure. The contamination from squark decays to charginos is statistically removed by plotting the distribution for $e^+e^- + \mu^+\mu^-$ pairs minus the same for $e^\pm\mu^\mp$ pairs. Reprinted from the ATLAS Technical Design Report.

Exercise *Consider a chain of two-body decays, $A \to bB \to bcC \to bcdD$, where b, c, d are massless particles. Show that the kinematic end point of the invariant mass $m(bcd)$ is given by,*

$$m(bcd)^2 \leq max\left[\frac{(m_A^2 - m_B^2)(m_B^2 - m_C^2)}{m_B^2}, \frac{(m_A^2 - m_C^2)(m_C^2 - m_D^2)}{m_C^2}, \frac{(m_A^2 m_C^2 - m_B^2 m_D^2)(m_B^2 - m_C^2)}{m_B^2 m_C^2}\right],$$

except for mass ranges where the absolute end point

$$m(bcd) = m_A - m_D$$

can be saturated.

This is in contrast to the case of the three-body decay of $A \to bB \to bcC$ where the saturation of the end point $m_A - m_C$ is possible only if $m_B^2 = m_A m_C$.

---

https://doi.org/10.1017/9781009289801.016 Published online by Cambridge University Press

To further facilitate pairing of jets with dileptons consistent with the decay chain (15.14), we focus on events with one $\ell^+\ell^- q$ invariant mass pairing above 600 GeV and the other below 600 GeV. There are two possible pairings of the jet with the leptons. If we define ℓ_1 to be the lepton that emerges promptly from decay of $\widetilde{Z}_2$, and ℓ_2 the one from the decay of the slepton, we have

$$m(\ell_1 q) < m_{\tilde{q}} \sqrt{1 - \frac{m^2_{\widetilde{Z}_2}}{m^2_{\tilde{q}}}} \sqrt{1 - \frac{m^2_{\tilde{\ell}}}{m^2_{\widetilde{Z}_2}}} = 479.3 \text{ GeV}, \tag{15.16a}$$

and

$$m(\ell_2 q) < m_{\tilde{q}} \sqrt{1 - \frac{m^2_{\widetilde{Z}_2}}{m^2_{\tilde{q}}}} \sqrt{1 - \frac{m^2_{\widetilde{Z}_1}}{m^2_{\tilde{\ell}}}} = 407.4 \text{ GeV}. \tag{15.16b}$$

The problem, of course, is even if the jet can be perfectly associated with the leptons, there is an ambiguity about which of the two leptons in an event is ℓ_1. The distribution of the larger of the two $m(\ell q)$ values for each event (using the jet which gives the lowest $m(\ell^+\ell^- q)$ value) is plotted in Fig. 15.14. For our case, this is bounded by (15.16a). The upper edge is not very sharp, but fits to the endpoint come within a few percent of its value. The other mass edge (15.16b) is buried under this distribution.

The three mass edges in the figures constrain, but do not determine, the four masses. To pin these down, we need a fourth mass edge. Unfortunately, except for effects of cuts, the lower edges of these distributions start at $m = 0$ and so provide no information. However, by focussing on events with a minimum value of $m(\ell_1\ell_2)$, we preclude the configuration with $m(q\ell_1\ell_2) = 0$, and the $m(q\ell_1\ell_2)$ distribution starts at a mass value depending on our choice of $m(\ell_1\ell_2)_{\min}$. The corresponding $m(\ell\ell q)$ distribution for events with

$$m(\ell^+\ell^-) > m(\ell^+\ell^-)_{\max}/\sqrt{2}$$

is shown in Fig. 15.15, where the larger of the two $m(\ell^+\ell^- q)$ values is plotted. A lower edge is clearly visible. The expression for this lower edge in terms of the sparticle masses and $m(\ell^+\ell^-)_{\min}$ is complicated and will not be reproduced here. For the present case, the theoretical edge is expected to be at 271.8 GeV, and appears to be smeared to lower values, perhaps because of energy lost to QCD radiation. The main point of this discussion is that at least for the case of a chain of two-body decays considered here, it is possible to extract the four mass values in a *model-independent* manner. Explicit fits to these quantities give sparticle masses to

https://doi.org/10.1017/9781009289801.016 Published online by Cambridge University Press

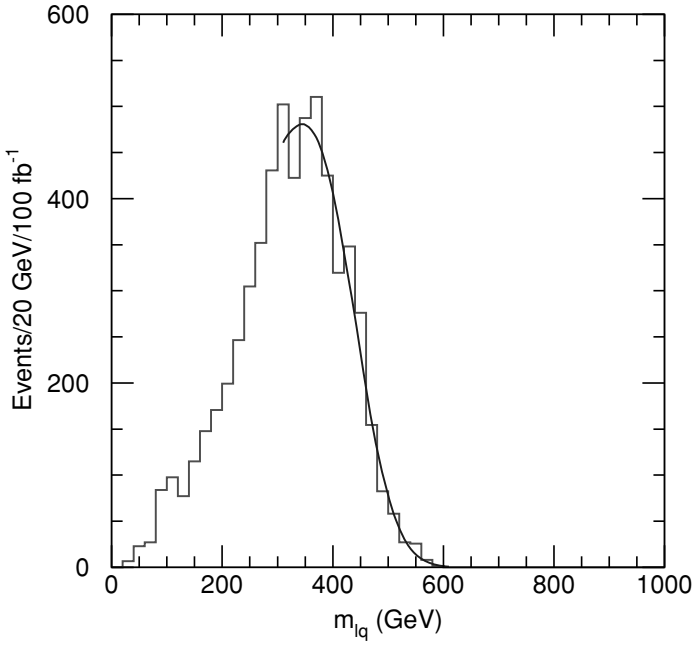

Figure 15.14 Distribution in $m(\ell q)$ for the smaller of the two $\ell^+\ell^- q$ invariant mass combinations for the mSUGRA point under study. Once again, the contamination from squark decays to chargino are removed by using the flavor weighted combination $e^+e^- + \mu^+\mu^- - e^{\pm}\mu^{\mp}$. Reprinted from the ATLAS Technical Design Report.

3–12%.[19] It is not surprising that $m_{\widetilde{Z}_1}$ has the largest error, since it is much smaller than the squark mass, and enters only (quadratically) via kinematics.

For the mSUGRA point used in the above example, the decay $\widetilde{Z}_2 \to h\widetilde{Z}_1$ occurs with a branching fraction of about 50%. We would thus expect that a data sample consisting mainly of SUSY events would contain a significant fraction of events that contain a high p_T Higgs boson h from cascade decays. Since h mostly decays via $h \to b\bar{b}$, such events would contain at least two b-quark jets whose presence is signaled by displaced vertices from B-meson decay, and which have a bump in their invariant mass distribution around the value of m_h; this is illustrated in Fig. 15.16. In general, if h is produced at significant rates in SUSY cascade decay events, it may well first be discovered as a $b\bar{b}$ mass bump in the SUSY event sample! Detection of the $h \to \gamma\gamma$ mode, which may take several years of LHC operation to establish,

[19] If all four sparticle masses can indeed be fit, the ambiguities in the formulae for the end points that we had referred to earlier would automatically be resolved.

https://doi.org/10.1017/9781009289801.016 Published online by Cambridge University Press

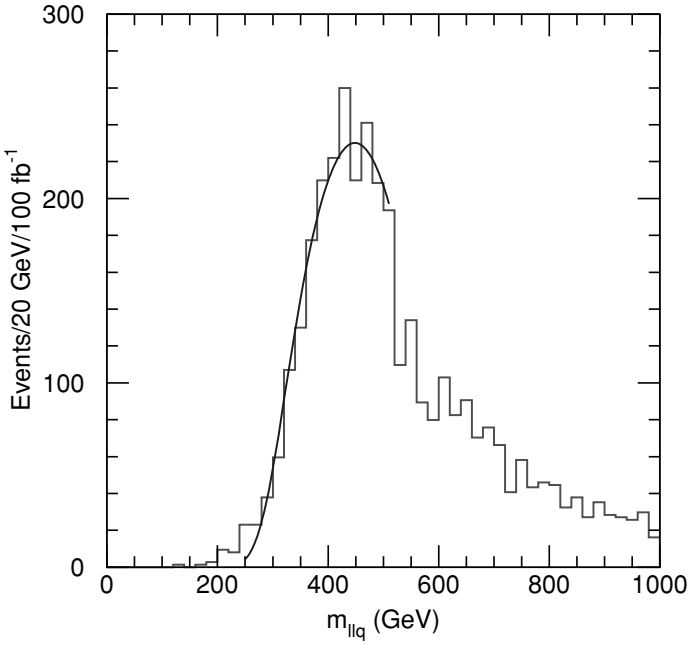

Figure 15.15 Distribution in $m(\ell^+\ell^- q)$ for the larger of the two $\ell^+\ell^- q$ invariant mass combinations for the mSUGRA model parameters in Fig. 15.11, but with the additional requirement that $m(\ell^+\ell^-) > m(\ell^+\ell^-)_{\max}/\sqrt{2}$. Reprinted from the ATLAS Technical Design Report.

is nonetheless very important because the location of the peak in the two-photon distribution yields a very accurate measurement of m_h.

These events may also allow the reconstruction of the decay chain

$$\tilde{q}_{\rm L} \to q\widetilde{Z}_2 \to qh\widetilde{Z}_1 \to qb\bar{b}\widetilde{Z}_1.$$

Since gluinos are heavier than squarks, $\tilde{q}_{\rm L}$ comes from either direct production, or from the decay of a gluino. A relatively clean sample may be obtained by focussing on events with just two hard jets (which most likely come from squark decay) and a pair of b-jets. The $m(b\bar{b}j)$ mass distribution from this chain must have both upper and lower end points that can be fixed in terms of $m_{\tilde{q}_{\rm L}}$, $m_{\widetilde{Z}_2}$, $m_{\widetilde{Z}_1}$, and m_h.

Exercise *Show that the end points of the $b\bar{b}j$ mass distribution from the cascade decay chain $\tilde{q}_{\rm L} \to q\widetilde{Z}_2 \to qh\widetilde{Z}_1 \to qb\bar{b}\widetilde{Z}_1$ are given by,*

$$m^2(b\bar{b}j)^{\rm max}_{\rm min} = m^2_{\tilde{q}} + m^2_{\widetilde{Z}_1} - 2E_{\tilde{q}}E_{\widetilde{Z}_1} \pm 2p_{\tilde{q}}p_{\widetilde{Z}_1},$$

https://doi.org/10.1017/9781009289801.016 Published online by Cambridge University Press

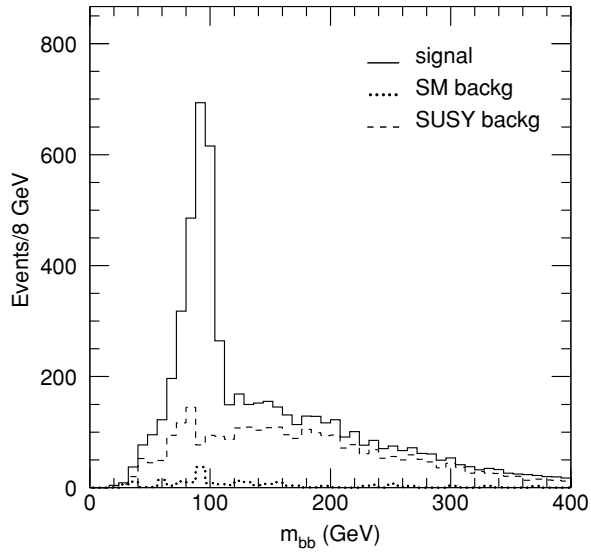

Figure 15.16 Distribution in $m(b\bar{b})$ for signal (solid) and SM (dots) and SUSY background (dashes) for the mSUGRA model with parameters as in Fig. 15.11, assuming an integrated luminosity of 30 fb^{-1}. Reprinted from the ATLAS Technical Design Report.

where

$$E_{\tilde{q}} = \frac{m_{\tilde{q}}^2 + m_{\widetilde{Z}_2}^2}{2m_{\widetilde{Z}_2}} \quad \text{and} \quad E_{\widetilde{Z}_1} = \frac{m_{\widetilde{Z}_2}^2 + m_{\widetilde{Z}_1}^2 - m_h^2}{2m_{\widetilde{Z}_2}}$$

are the energies of the squark and $\widetilde{Z}_1$ *in the rest frame of* $\widetilde{Z}_2$, $p_{\tilde{q}} = \sqrt{E_{\tilde{q}}^2 - m_{\tilde{q}}^2}$, *and* $p_{\widetilde{Z}_1} = \sqrt{E_{\widetilde{Z}_1}^2 - m_{\widetilde{Z}_1}^2}$.

Show that the ideal $m(b\bar{b}j)$ *spectrum for the mSUGRA model that we have been examining (where* $m_{\tilde{q}} = 688$ *GeV,* $m_{\widetilde{Z}_2} = 233$ *GeV,* $m_{\widetilde{Z}_1} = 122$ *GeV, and* $m_h = 93$ *GeV) extends from 338 GeV to 524 GeV. Compare this with the* $m(b\bar{b}j)$ *distributions in the ATLAS Technical Design Report, where effects of detector resolution and jet misidentification have been included. Although the distributions are smeared particularly at the lower end point, it may be possible to make corrections to compensate energy losses in b-jets due to escaping neutrinos or losses outside the cone once LHC data are available. Moreover, a more thorough analysis may better isolate events with Higgs bosons.*

https://doi.org/10.1017/9781009289801.016 Published online by Cambridge University Press

Once sparticle mass spectra have been extracted from the various reconstructed mass edges, it is natural to check whether these are consistent with any of the models that we have considered in Chapter 11. If a good fit is obtained, it would be possible to extract the underlying parameters. Indeed, for the model that we have been examining, it has been claimed in the ATLAS Technical Design Report that m_0, $m_{1/2}$, and $\tan\beta$ can be extracted with a precision of 2–5% with an integrated luminosity of just 30 fb^{-1}.

Our discussion of mass measurements is only to give the reader a flavor of what might be possible, and is not intended to be either comprehensive or complete. In fact, examination of the prospects for precision measurements at the LHC has only recently begun, and much work remains to be done in this direction. Here, we highlight a few more interesting results, and refer the reader to the literature for more details.

- We saw how it might be possible to check for consistency of the data with the mSUGRA model, and to extract some of the underlying parameters. It may be that the universality assumption is violated. It would be possible to distinguish some classes of models with non-universal SSB parameters from mSUGRA.
- If $\tan\beta$ is large so that decays of charginos and neutralinos to tau leptons become dominant, it may still be possible to reconstruct various mass edges, though with somewhat degraded precision.
- In GMSB models with prompt decay of a bino-like NLSP, the decay chain $\widetilde{Z}_2 \to \tilde{\ell}^{\pm}\ell^{\mp} \to \ell^+\ell^-\widetilde{Z}_1 \to \ell^+\ell^-\gamma\tilde{G}$ has the same number of steps as the decay chain from $\tilde{q}_{\rm L}$ decays for the mSUGRA case discussed above, and so can be similarly analyzed. An important difference is that at least for the case study in the ATLAS Technical Design Report, both the $m(\ell_1\gamma)$ as well as the $m(\ell_2\gamma)$ edges can be clearly distinguished in the $m(\ell\gamma)$ distribution. The invariant mass edges of $\ell^+\ell^-$, $\ell_1\gamma$, $\ell_2\gamma$, and $\ell^+\ell^-\gamma$ distributions are sufficient to determine $m_{\widetilde{Z}_2}$, $m_{\tilde{\ell}}$, and $m_{\widetilde{Z}_1}$ to high accuracy. Squark and gluino mass reconstruction is also possible. These measurements allow determination of some of the underlying model parameters: Λ can be determined at the couple of percent level, and, for the case examined, even the messenger scale can be extracted within $\pm 40\%$. If instead, the $\widetilde{Z}_1$ decay is long lived and decays outside the detector, the analysis will be similar to those described above for the mSUGRA model.
- The intermediate possibility that the $\widetilde{Z}_1$ NLSP decays with a decay length of 10 cm to 20 m allows other interesting measurements. If the photon from $\widetilde{Z}_1$ converts to an electron pair, its momentum and point of origin can be well determined, and reconstruction of the entire event appears to be possible.[20] Of course, it is only in a fraction of events that the photon converts. These authors have claimed

[20] See K. Kawagoe, T. Kobayashi, M. Nojiri and A. Ochi, *Phys. Rev.* **D69**, 035003 (2004).

https://doi.org/10.1017/9781009289801.016 Published online by Cambridge University Press

that reconstruction is also possible even in events where the photon does not convert: the degradation of the precision is partially compensated by the larger number of these events. Finally, in such scenarios, the lifetime of the NLSP can be determined to within a few percent. This is a very important measurement because the NLSP lifetime is simply related to the fundamental SUSY breaking scale.

- The GMSB case with a slepton co-NLSP has also been examined in the ATLAS Technical Design Report.[21] If $\tilde{\ell}_R$ is quasi-stable and has a distinct track, neutralinos decaying via $\widetilde{Z}_i \to \ell\tilde{\ell}_R$ show up as clear mass peaks in appropriate distributions. The decays $\tilde{\ell}_L \to \ell\widetilde{Z}_1$ can be used to reconstruct $m_{\tilde{\ell}_L}$. For the case of prompt NLSP decays $\tilde{\ell}_R \to \ell\tilde{G}$, it has been shown that a variety of mass edges involving dileptons and jets can be reconstructed, giving good fits to model parameters. Once again, the underlying model parameters can be extracted. The precision that can be attained is significantly better if the slepton NLSP is quasi-stable. In this case, a determination of the fundamental SUSY breaking scale (via the slepton lifetime) with a precision of tens of percent is possible if the slepton decay length is between $\sim$0.5 m and 1 km.

15.5.2 Precision measurements at an LC

If the discovery of new physics is established, the next step will be to figure out what it is. Taking this new physics to be supersymmetry, this may come about by the discovery of several superpartners. At the LHC, the discovery of several superpartners might occur if signals for new physics in many different channels can be interpreted as different cascade decay chains from superparticle pair production, or via the identification of several "kinematic edges" in appropriate distributions as we have just discussed. Logically, of course, such an observation would only establish the discovery of several new particles. The magnitude of the signal cross sections would tell us whether or not the new particles exhibit strong interactions, and maybe even indicate some of their other gauge quantum numbers.

If superpartners are accessible at linear colliders, the cleanliness of the initial and final states frequently allows their properties to be straightforwardly determined.[22] Since SUSY predicts the existence of superpartners with spins differing by one half, we will first outline how the spin of any new particle may be determined. We will then discuss how sparticle masses may be determined, since these encode the information about the all-important (and as yet completely unknown) mechanism by

[21] See also S. Ambrosanio *et al.*, *JHEP* **01**, 014 (2001) and hep-ph/0012192 (2000).

[22] Studies of the capabilities of linear colliders for SUSY measurements were pioneered by T. Tsukamoto *et al.*, *Phys. Rev.* **D51**, 3153 (1995). H. Baer *et al.*, *Phys. Rev.* **D54**, 6735 (1996) included the effects of cascade decays in the analysis of SUSY mass measurements, and M. Nojiri *et al.*, *Phys. Rev.* **D54**, 6756 (1996) discussed the determination of the properties of third generation sleptons.

https://doi.org/10.1017/9781009289801.016 Published online by Cambridge University Press

which superpartners of SM particles obtain their masses: within specific models, information about the sparticle spectrum may allow us to infer some of the underlying model parameters. If the Higgs bosons A, H or $H^{\pm}$ are also kinematically accessible, we will see that LC experiments will allow further tests of the MSSM framework, and may also yield further information about underlying parameters that may be more difficult to get at otherwise. However, to unambiguously establish (in a model-independent manner) that any new physics is softly broken supersymmetry, we have to show that the dimensionless couplings of the new particles are (aside from radiative corrections) equal to the corresponding SM couplings. We will illustrate the extent to which such a determination is possible in experiments at an e^+e^- LC.

Spin determination

If sparticle production dominantly occurs via the exchange of vector bosons in the s-channel, it is easy to see from Appendix A.2 that the sparticle angular distribution is given by

$$\sin^2\theta$$

for spin 0 particles, and by

$$E^2(1+\cos^2\theta)+m^2\sin^2\theta$$

for equal mass spin $\frac{1}{2}$ particles. If the sparticles are produced with a sufficient boost, the angular distribution of their daughters will be strongly correlated with that of the parent sparticles; the differences between the angular distributions should suffice to readily distinguish between the spin zero and spin $\frac{1}{2}$ cases. An integrated luminosity of several tens of fb^{-1} should suffice to establish the spin 0 nature of smuons at a 500 GeV LC.

We mention in passing that angular distributions may also contain dynamical information. For instance, in $e^+e^- \to \tilde{e}_{\mathrm{L(R)}}\bar{\tilde{e}}_{\mathrm{L(R)}}$ processes, selectrons (anti-selectrons) will preferentially be produced along the electron (positron) beam direction if t-channel neutralino exchanges are important, resulting in an angular asymmetry in the distribution of the daughter electron.

Exercise *Consider the reaction $e^+e^- \to \tilde{\mu}_{\mathrm{R}}\bar{\tilde{\mu}}_{\mathrm{R}} \to \mu^+\mu^-\widetilde{Z}_1\widetilde{Z}_1$ at a LC, where $\tilde{\mu}_{\mathrm{R}} \to \mu\widetilde{Z}_1$. We will see in the next subsection that it is possible to extract $\tilde{\mu}_{\mathrm{R}}$ and $\widetilde{Z}_1$ masses from this process. Using the fact that the smuon is a narrow state, show that it is then possible to completely reconstruct (up to a quadratic ambiguity) the smuon momenta from the observable momenta of the final state muons and the missing three-momentum vector, even though each event contains two escaping neutralinos. In this sense, the angular distribution of smuons can be experimentally constructed.*

---

https://doi.org/10.1017/9781009289801.016 Published online by Cambridge University Press

Mass determination

If sparticles are discovered, determination of their masses will be one of the highest priorities. Measurements at the LHC will, as we have seen, provide some information but at LCs it will be possible to have a systematic program for sparticle spectroscopy. In the approach, initiated by the Japanese Linear Collider group, the idea is to exploit the kinematics of the decays to infer the masses. This is not straightforward since every SUSY event contains two LSPs that escape detection so that a reconstruction of "mass bumps" is not possible.[23] For the production of spinless particles p_1 and p_2 via $e^+e^- \to p_1 + p_2$, followed by the decay $p_2 \to p_3 + p_4$, it is straightforward to check that the energy spectrum of the particle p_3 is flat and kinematically restricted to be between

$$\gamma(E_3^* - \beta p_3^*) \le E_3 \le \gamma(E_3^* + \beta p_3^*), \tag{15.17}$$

where $E_3^* = (m_2^2 + m_3^2 - m_4^2)/2m_2$, $p_3^* = \sqrt{E_3^{*2} - m_3^2}$, $\gamma = E_2/m_2$, $\beta = \sqrt{1 - 1/\gamma^2}$, and $E_2 = (s + m_2^2 - m_1^2)/2\sqrt{s}$, up to corrections from energy mis-measurements, particle losses and bremsstrahlung and beamstrahlung effects.

These considerations can be directly applied to slepton pair production, since sleptons decay via two-body modes. In the case that the sleptons can only decay via $\tilde{\ell} \to \ell \widetilde{Z}_1$, the end points of the energy distribution of the final state lepton depend only on the values of $m_{\tilde{\ell}}$ and $m_{\widetilde{Z}_1}$ via kinematics. Since sharp end points can be determined rather precisely, it is possible to infer the slepton and neutralino masses.

To illustrate this, we show the muon energy distribution from $e^+e^- \to \tilde{\mu}_R \bar{\tilde{\mu}}_R \to \mu^+\mu^- \widetilde{Z}_1 \widetilde{Z}_1$ production in Fig. 15.17*a*, which is taken from the simulation by Tsukamoto *et al.* In this study, the right-handed charged slepton is the NLSP with $m_{\tilde{\ell}_R} = 141.9$ GeV, and decays to the neutralino which has a mass $m_{\widetilde{Z}_1} = 117.8$ GeV. Charginos have a mass $m_{\widetilde{W}_1} = 219.3$ GeV and so cannot be produced at the assumed center of mass energy of 350 GeV. By choosing the electron beam to be mainly right-handed, the dominant WW background to the acolinear muon pair signal is greatly diminished, while the right-slepton pair production cross section is enhanced. The data points correspond to a Monte Carlo expectation for an integrated luminosity of just 20 fb^{-1}, while the solid curve is the "best fit" to these data. The corresponding error contours are shown in 15.17*b*. We see that $m_{\tilde{\mu}_R}$ and $m_{\widetilde{Z}_1}$ can both be determined to about 1%. These sparticle masses serve as inputs for determining the smuon spin, as discussed above. In addition, by varying the beam

[23] It may be possible to reconstruct mass bumps in R-parity violating scenarios, depending on how the LSP decays.

https://doi.org/10.1017/9781009289801.016 Published online by Cambridge University Press

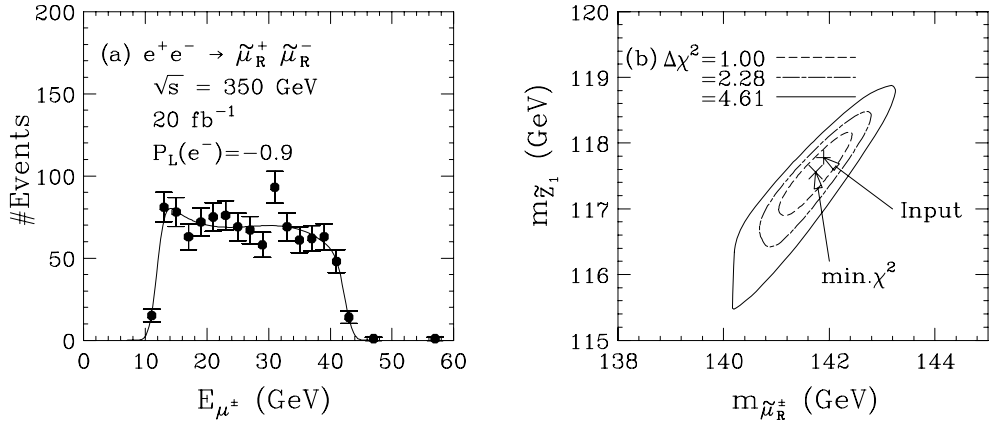

Figure 15.17 (*a*) The energy distribution of final state muons from $e^+e^- \to \tilde{\mu}_R^+\tilde{\mu}_R^- \to \mu^+\mu^-\widetilde{Z}_1\widetilde{Z}_1$ at $\sqrt{s} = 350$ GeV with $P_L(e^-) = -0.9$, within the mSUGRA framework with $m_0 = 70$ GeV, $M_2 = 250$ GeV, $\mu = 400$ GeV, $A_0 = 0$, and $\tan\beta = 2$. The data points are from Monte Carlo while the smooth curve is from a fit. In (*b*) are shown error contours from a two-parameter fit to $m_{\tilde{\mu}_R}$ and $m_{\widetilde{Z}_1}$. Reprinted with permission from T. Tsukamoto, K. Fujii, H. Murayama, M. Yamaguchi and Y. Okada, *Phys. Rev.* **D51**, 3153 (1995), copyright (1995) by the American Physical Society.

polarization and comparing to the cross section, the smuon weak isospin and hypercharge can be extracted, verifying that it is the right-superpartner of the muon. The $\tilde{\mu}_L$ mass and other quantum numbers should be measurable in a similar manner once threshold is passed for $\tilde{\mu}_L\bar{\tilde{\mu}}_L$ production.

The $\tilde{e}_R$ mass can be similarly measured to even better precision since it has a larger cross section because of t-channel neutralino exchange contributions whose presence, as we have noted, will also be reflected in the angular distribution. For selectrons, $\tilde{e}_R\bar{\tilde{e}}_L$, $\bar{\tilde{e}}_R\tilde{e}_L$, and $\tilde{e}_L\bar{\tilde{e}}_L$ may also be accessible, each with unique energy edges in the electron or positron energy distributions. Variable beam polarization will be a key tool in discriminating the different reactions. If we assume that the LSP is dominantly a hypercharge gaugino and that gaugino masses satisfy the unification condition, it should be possible to roughly project the chargino threshold even before charginos are discovered.

Although Tsukamoto *et al.* had confined their analysis to cases where sparticles directly decay to the LSP, it was shown shortly after that cascade decays do not degrade the precision with which sparticle masses can be determined.[24] On the contrary, these decays provide new opportunities: for instance, if the decay $\tilde{\nu}_e \to e\widetilde{W}_1$ has a significant branching ratio, a determination of the end points of the electron

[24] H. Baer *et al.*, *Phys. Rev.* **D54**, 6735 (1996).

https://doi.org/10.1017/9781009289801.016 Published online by Cambridge University Press

energy spectrum from $e^+e^- \to \tilde{\nu}_e + \tilde{\nu}_e \to e\widetilde{W}_1 + e\widetilde{W}_1 \to e\mu\nu_\mu\widetilde{Z}_1 + ejj\widetilde{Z}_1$ yields information about electron sneutrino and chargino masses, with a precision at about the percent level. In this case, of course, chargino pair production is also kinematically accessible and, as discussed below, will probably be how the chargino mass will first be determined. Obtaining this same value for $m_{\widetilde{W}_1}$ in $\tilde{\nu}_e\tilde{\nu}_e$ events will be direct evidence for chargino production in SUSY decay cascades. Masses of muon and tau sneutrinos are more difficult to extract since these are produced only via s-channel Z exchange, and so have smaller production cross sections (see Fig. 12.32). We will revisit this later.

The end-point technique that we have just been describing has also been applied to the lighter stau, assuming $\tilde{\tau}_1 \to \tau\widetilde{Z}_1$.[25] In this case, the situation is complicated by the fact that a part of the tau energy is carried off by the tau neutrino, so that the end points of the tau energy spectrum are smeared. Nonetheless, from the spectrum of visible energy of taus decaying via $\tau \to \rho\nu$, it is possible to obtain $m_{\tilde{\tau}_1}$ with a precision of $\sim 2\%$, assuming an integrated luminosity of ~ 100 fb^{-1}. Including tau decays to π and a_1 would improve the precision by about a factor of two.

Tau sleptons differ from other sleptons in that they are expected to have significant mixing between left- and right-states: $\tilde{\tau}_1 = \tilde{\tau}_\mathrm{L}\cos\theta_\tau - \tilde{\tau}_\mathrm{R}\sin\theta_\tau$. The stau pair production cross section is sensitive to the mixing angle. In Fig. 15.18, we show the result of a simulation to illustrate that the stau mass and mixing angle can be determined to a few percent at a LC. While the fact that taus are unstable was an undesirable complication for stau mass determination, it is now a boon because the energy spectrum of the daughter tau neutrino (and hence of the visible hadronic decay products) is sensitive to the polarization of the tau. Since the tau polarization depends on the stau mixing angle, a study of stau production provides information not accessible in selectron or smuon production (because polarizations of final state electrons and muons are not measured). The tau polarization can be sensitive to the parameter $\tan\beta$, especially in the case where the $\widetilde{Z}_1$ contains a significant higgsino component. In this case, the $\widetilde{Z}_1$ coupling to the tau–stau system also depends on the tau Yukawa coupling. Then, by simultaneously studying selectron pair production (to constrain neutralino mixings) and stau pair production, it may be possible to determine $\tan\beta$.

If charginos are the lightest charged sparticles, it is likely that they will be discovered before sleptons. If the chargino decays via the two-body mode, $\widetilde{W}_1 \to W\widetilde{Z}_1$ and both Ws decay hadronically, it is straightforward to reconstruct each W from the invariant mass of the jets. Aside from spin correlation effects, the chargino and LSP mass can then be obtained via two-body kinematics from the

[25] M. Nojiri *et al.*, *Phys. Rev.* **D54**, 6756 (1996).

https://doi.org/10.1017/9781009289801.016 Published online by Cambridge University Press

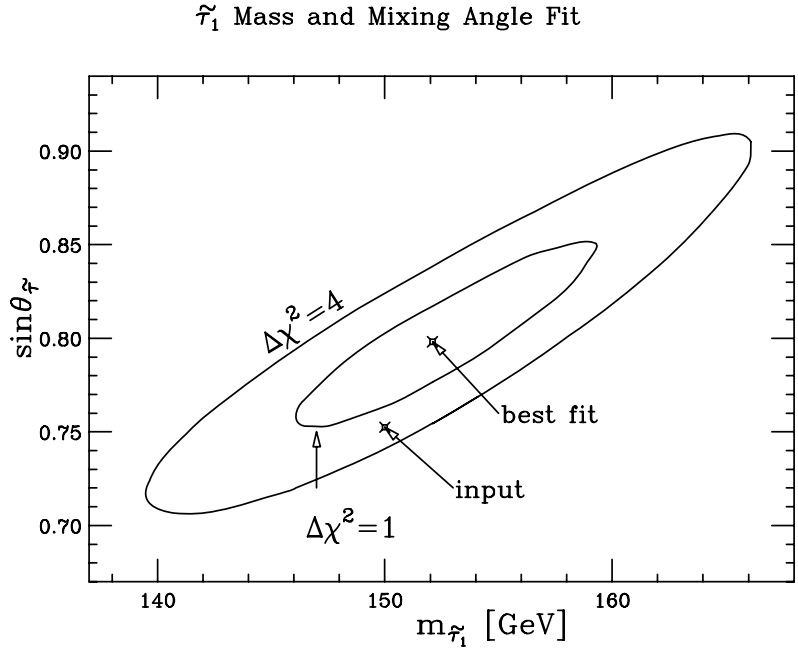

Figure 15.18 Error ellipses from a two-parameter fit to the stau mass and mixing angle. In this illustration, 5000 stau pairs were simulated at $\sqrt{s} = 500$ GeV, assuming that the stau of mass 150 GeV decays exclusively to a 100 GeV neutralino. The stau mixing angle is taken to be given by $\sin\theta_\tau = 0.7526$. A SM background corresponding to an integrated luminosity of 100 fb^{-1} is also included. For more details, we refer the reader to M. Nojiri, K. Fujii and T. Tsukamoto, *Phys. Rev.* **D54**, 6756 (1996), copyright (1996) by the American Society, from which this figure is reprinted with permission.

energy distribution of the W, as in the case of the slepton. An mSUGRA case study by Tsukamoto *et al.* showed that the mass of a chargino as heavy as 220 GeV could be extracted to within a few percent at a 500 GeV LC, assuming an integrated luminosity of 50 fb^{-1}.

What if the chargino decays via three-body decays? In this case, we can force quasi-two-body kinematics by dividing the sample of $e^+e^- \to \widetilde{W}_1^+\widetilde{W}_1^- \to jj\widetilde{Z}_1 + \ell\nu\widetilde{Z}_1$ events, enriched in signal via suitable cuts, into several narrow bins in m_{jj}.[26] For each m_{jj} bin, the E_{jj} distribution follows the form for $\widetilde{W}_1 \to \widetilde{Z}_1 W^*$ decays, with M_{W^*} close to the central value of the chosen bin. The result of such an analysis is shown in Fig. 15.19 for an mSUGRA model with $m_0 = 300$ GeV, $m_{1/2} = 150$ GeV, $A_0 = -600$ GeV, $\tan\beta = 2$, and $\mu > 0$. The upper frame shows the error ellipse obtained by combining the analyses of the E_{jj} distributions for four different m_{jj}

[26] For details, see H. Baer, R. Munroe and X. Tata, *Phys. Rev.* **D54**, 6735 (1996) where this technique is discussed.

https://doi.org/10.1017/9781009289801.016 Published online by Cambridge University Press

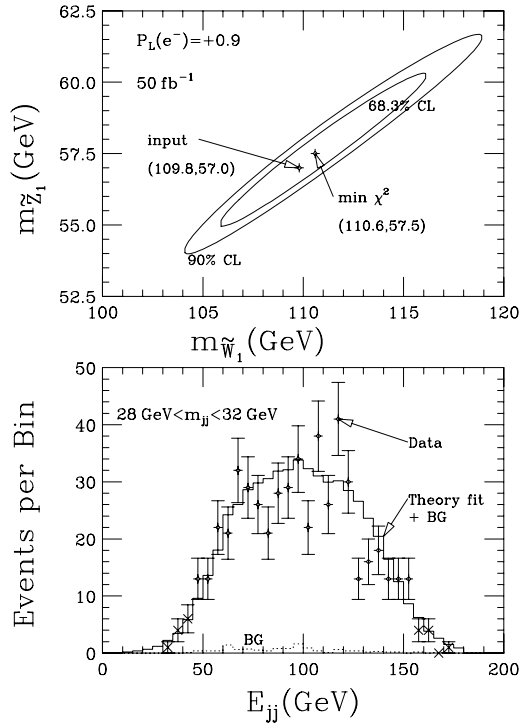

Figure 15.19 The upper frame shows the error ellipses obtained from an analysis of $jj\ell + E_{\rm T}^{\rm miss}$ events from chargino pair production with forced two-body kinematics, after combining the analysis from four different m_{jj} bins, as discussed in the text. The lower frame shows the $E_{W^*} = E_{jj}$ distribution for $M_{W^*} = 30 \pm 2$ GeV. Reprinted with permission from H. Baer, R. Munroe and X. Tata, *Phys. Rev.* **D54**, 6735 (1996), copyright (1996) by the American Physical Society.

bins, while the lower frame shows one of these E_{jj} distributions. The result includes SM backgrounds and contamination to the $\ell jj + E_{\rm T}^{\rm miss}$ signal from other SUSY sources. Once again, we see that a few percent determination of the chargino and LSP mass should be possible at a LC. The precision obtained here is comparable to that obtained by Tsukamoto *et al.* by fitting the shape of the E_{jj} distribution for charginos decaying via three-body decays. It is worth mentioning that for model parameters in the HB/FP region (which yields a favorable value for the neutralino relic density), this technique will be applicable.

In the event that $e^+e^- \to \widetilde{Z}_1\widetilde{Z}_2$ is the only SUSY reaction accessible, mass measurements may still be possible, as illustrated in Fig. 15.20. In this case, $\widetilde{Z}_2 \to \widetilde{Z}_1 h$, $h \to b\bar{b}$, and the missing mass distribution in $b\bar{b} + \not{E}$ events allows $m_{\widetilde{Z}_2}$ and $m_{\widetilde{Z}_1}$ to be determined to a few percent, provided m_h has previously been determined. The missing mass distribution is better suited than the E_{bb} distribution for this

https://doi.org/10.1017/9781009289801.016 Published online by Cambridge University Press

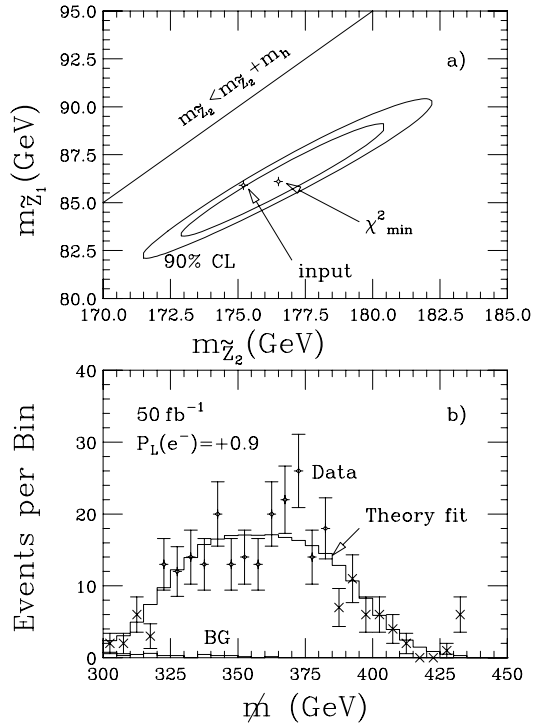

Figure 15.20 Error ellipses and missing mass distributions for $b\bar{b} + \not{E}$ events in a simulation including $\widetilde{Z}_1\widetilde{Z}_2$ production. Reprinted with permission H. Baer, R. Munroe and X. Tata, *Phys. Rev.* **D54**, 6735 (1996), copyright (1996) by the American Physical Society.

measurement because in the determination of missing mass, mismeasurement and losses from undetected neutrinos partially cancel out.

Squark pairs may also be produced in e^+e^- collisions. In many models, the lightest top squark is expected to be the lightest of all squarks, and hence the most likely to be accessible to linear collider searches. Linear collider event generation studies have been performed for an mSUGRA point with $m_{\tilde{t}_1} = 180$ GeV. The signal from $\tilde{t}_1\bar{\tilde{t}}_1$ pair production with $\tilde{t}_1 \to b\widetilde{W}_1$ decay can be almost completely separated from SM backgrounds by requiring ≥ 5 jet events including at least two b-jets. The b-jet energy distribution depends on $m_{\tilde{t}_1}$ and $m_{\widetilde{W}_1}$, and a two-parameter fit gives a measure of these masses to about 5%, as can be seen from Fig. 15.21. By making full use of beam polarization and other capabilities of the LC, it appears that it is possible to also determine the top squark mixing angle to a few percent.[27]

[27] R. Keranen, A. Sopczak, H. Nowak and M. Berggren, *Eur. Phys. J.* **C7**, 1 (2000).

https://doi.org/10.1017/9781009289801.016 Published online by Cambridge University Press

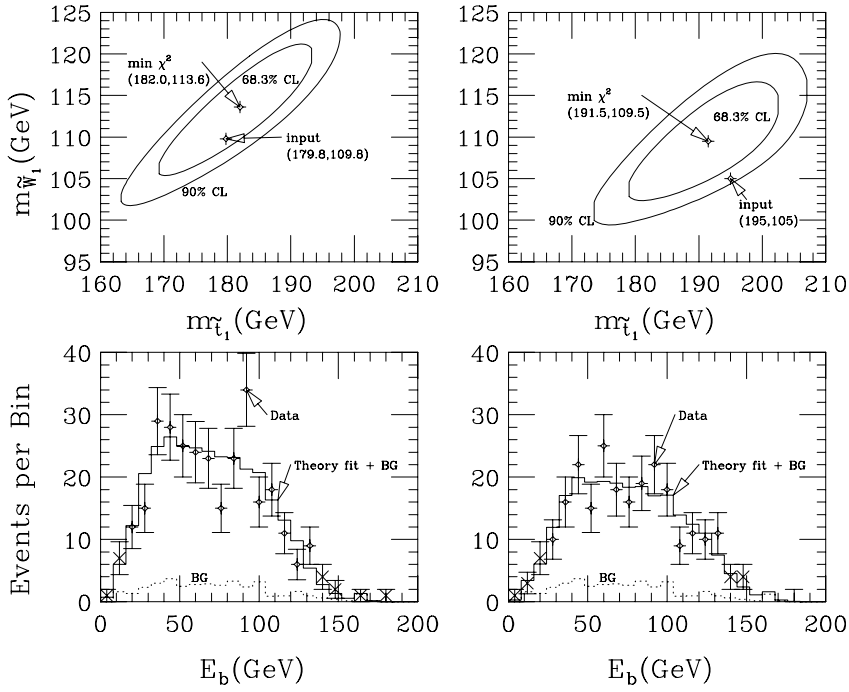

Figure 15.21 Error ellipses for a two-parameter fit to $m_{\tilde{t}_1}$ and $m_{\tilde{W}_1}$ for two nearby parameter space points where $\tilde{t}_1$ pair production is accessible. The corresponding b-jet energy distributions are also shown. Reprinted with permission from H. Baer, R. Munroe and X. Tata, *Phys. Rev.* **D54**, 6735 (1996), copyright (1996) by the American Physical Society.

If pair production of heavier squarks is also kinematically accessible, an LC would be ideal for performing squark spectroscopy. Aside from kinematic determinations of the type that we have been describing, we can see from (A.21a) that by adjusting the polarization of the electron beam, it is also possible to alternate between signals from $\tilde{q}_R\bar{\tilde{q}}_R$ or $\tilde{q}_L\bar{\tilde{q}}_L$ pairs, depending on beam polarization.[28]

It has been suggested that an energy scan of the sparticle production cross section near the production threshold offers a more precise determination of sparticle masses than the "kinematic" measurements described above. The idea is very simple. The shape of the cross section for sparticle pair production close to threshold is a simple function of just the sparticle mass, so that by determining this shape it should be possible to extract the mass very precisely. Indeed, it has been claimed that determining the cross section for ten values of energy each spaced apart by ~ 1 GeV leads to a precision better than a part per mille (a percent) for the masses of

[28] See J. Feng and D. Finnel, *Phys. Rev.* **D49**, 2369 (1994).

https://doi.org/10.1017/9781009289801.016 Published online by Cambridge University Press

Table 15.3 *A summary of the projections for tau sneutrino mass measurements (90% CL) for two mSUGRA model cases, assuming a 95% longitudinally polarized electron beam. The first row shows the projection with backgrounds and SUSY contamination included, while the second shows the corresponding projection if these backgrounds can be effectively eliminated without loss of signal. For $\tilde{\nu}_e$, both SM background as well as SUSY contamination are insignificant.*

	Case I	Case II
$m_{\tilde{\nu}_\tau}$ (500 fb^{-1})	$153^{+12.5}_{-24}$ GeV	$174.9^{+7.1}_{-15.4}$ GeV
	$153^{+11.5}_{-24}$ GeV	$175.4^{+5.6}_{-10.9}$ GeV
$m_{\tilde{\nu}_e}$ (120 fb^{-1})	$157.8^{+0.8}_{-1.2}$ GeV	$178.0^{+0.5}_{-0.8}$ GeV
$m_{\tilde{\nu}_e}$ (500 fb^{-1})	$158.1^{+0.4}_{-0.5}$ GeV	$178.2^{+0.2}_{-0.4}$ GeV

$\tilde{\nu}_e$, $\tilde{e}$, and $\widetilde{W}_1$ ($m_{\tilde{\nu}_\tau}$, $m_{\tilde{\tau}_2}$), assuming an integrated luminosity of just 10 fb^{-1} for each energy scan. The problem is that in order to obtain a relatively background free sample of signal events which is essential for studying the threshold shape, one is forced to focus on particular final states. Not only does this lead to a reduction in the signal but, even more importantly, it also introduces an *unknown* branching fraction on which the cross section depends so that now both the mass as well as the branching fraction have to be extracted from the same counting experiment. This, in turn, leads to a significant degradation in the precision with which sparticle masses may be extracted.

The issue is not simply an academic one because precise determinations of (especially third generation) sparticle masses can provide important information about the underlying physics via which MSSM sparticles obtain their masses. An independent analysis by Mizukoshi *et al.*[29] concludes that the optimal way to make such a mass measurement is to divide the available luminosity between three or four energy points, one of which is chosen at the highest possible energy (this constrains the branching fraction), one close to the threshold and one somewhere in between.[30] The result of their analysis of the precision that is possible for sneutrino mass measurements in two different mSUGRA models is summarized in Table 15.3.

[29] J. K. Mizukoshi *et al.*, *Phys. Rev.* **D64**, 115017 (2001).
[30] Since it is not practical to perform a detailed scan of the energy threshold for every sparticle, this is a welcome conclusion. Indeed, running at intermediate values of energy may prove useful for many purposes.

https://doi.org/10.1017/9781009289801.016 Published online by Cambridge University Press

We see that while a precision approaching a part per mille may be possible for $m_{\tilde{\nu}_e}$, and perhaps also for $m_{\tilde{e}}$ and $m_{\widetilde{W}_1}$, an integrated luminosity of 500 fb^{-1} is required. For third generation sneutrinos, the precision is at best several percent.[31] It seems, therefore, that the precision from threshold scans and the kinematic measurements discussed previously is quite comparable.

The Higgs boson sector

The LC is an ideal facility for a study of the Higgs sector, especially if the energy is high enough to access states other than h. The MSSM Higgs boson sector is extremely constrained theoretically, so that precision measurements can serve to experimentally distinguish it from that of the SM, or perhaps exclude it altogether.

Direct observation of the heavier Higgs bosons of the MSSM not only establishes that there is physics beyond the SM, but provides new opportunities. For instance, combining the measurements of $4b$ production from $e^+e^- \to b\bar{b}A$, $b\bar{b}H$, and HA production processes, together with charged Higgs boson measurements, can lead to a determination of $\tan\beta$ to a high precision.[32] While a study of chargino and neutralino processes may also lead to a determination of $\tan\beta$ if it happens to be small, Higgs boson processes (and to some extent, precise determination of stau properties) offer the best hope for determining $\tan\beta$ when it is large.[33] If $\tan\beta$ is very large, it may also be possible to determine it from the measurements of the widths of the heavy Higgs bosons of the MSSM. Strictly speaking, what is determined are the Yukawa couplings. Although the Yukawa coupling is simply related to $\tan\beta$ at tree level, for large values of $\tan\beta$ one must be careful to include important radiative corrections to reliably extract its value.

If the heavier Higgs bosons are not directly accessible, a precise measurement of the branching ratios of h may still make it possible to exclude the SM, depending on the values of other parameters. For a discussion of these, as well as of many other important measurements possible in the Higgs sector (including a determination of their quantum numbers, couplings to gauge bosons, and their self-couplings), we refer the reader to the literature.

Establishing supersymmetry

The discovery of a few sparticle states will probably convince enthusiasts that nature is supersymmetric. To unambiguously establish that the new physics is indeed (softly broken) supersymmetry, it is necessary to show that the dimensionless couplings of the new particles are equal to the corresponding SM couplings. This

[31] We may expect that a determination of $m_{\tilde{\tau}_2}$ will have the same difficulties as that for $m_{\tilde{\nu}_\tau}$.

[32] See J. Gunion, T. Han, J. Jiang and A. Sopczak, *Phys. Lett.* **B565**, 42 (2003); see also V. Barger, T. Han and J. Jiang, *Phys. Rev.* **D63**, 075002 (2001).

[33] Recall that $\tan\beta$ enters via the mass matrices which really depend on $\sin\beta$ and $\cos\beta$, so that its determination becomes difficult if $\tan\beta$ is large.

https://doi.org/10.1017/9781009289801.016 Published online by Cambridge University Press

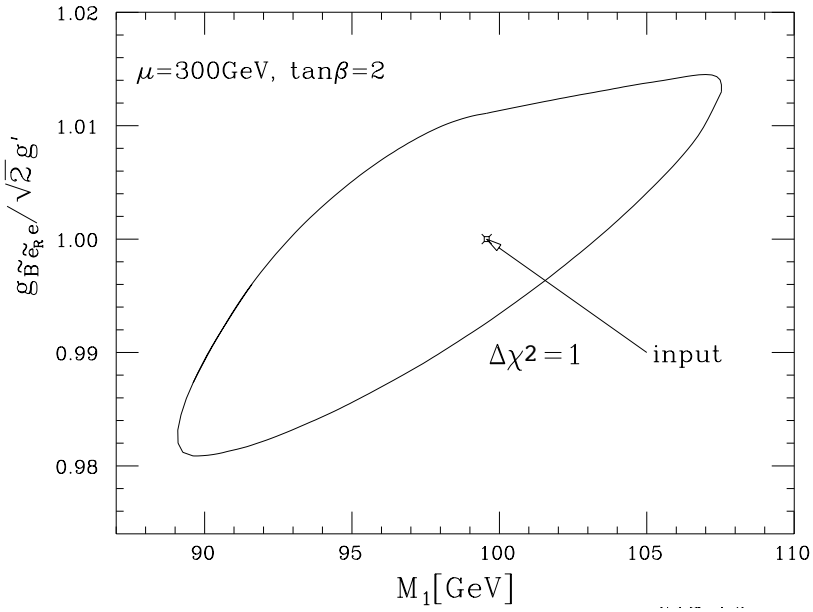

Figure 15.22 The $\Delta\chi^2 = 1$ contour to illustrate the precision with which the bino–selectron–electron coupling may be extracted in experiments at a linear collider from a study of selectron pair production. This study was performed within the framework of a SUSY model with $m_{\tilde{e}_R} = 200\,\text{GeV}$, $M_1 = 99.6\,\text{GeV}$, $\mu = 200\,\text{GeV}$, and $\tan\beta = 2$, and an integrated luminosity of $100\,\text{fb}^{-1}$ was assumed. We see that the ratio of couplings is determined to be unity at about the percent level. This figure is adapted from M. Nojiri, K. Fujii and T. Tsukamoto, *Phys. Rev.* **D54**, 6756 (1996), where more details about this analysis can be found. Reprinted with permission, copyright (1996) by the American Physical Society.

equality is a direct consequence of supersymmetry, and is independent of any underlying model. Radiative corrections from SUSY breaking effects result in small deviations from exact equality which, as we will see, encode information about sparticle masses. The situation is identical to that in spontaneously broken gauge theories in that (tree-level) relationships between dimensionless couplings implied by the symmetry continue to be preserved, while the corresponding relationships between masses may be badly violated.

Experiments at LCs provide a unique opportunity to test such relations if either sleptons or charginos are kinematically accessible.[34] For instance, at tree level, the coupling $g_{\tilde{B}\tilde{e}_R e}$ of the electron to the selectron–bino system is simply the SM hypercharge gauge coupling, aside from a symmetry coefficient of $\sqrt{2}$. Establishing this equality is complicated by the fact that the bino is not a mass eigenstate, so that mixing effects need to be disentangled. Nevertheless, by a careful analysis of $\tilde{e}_R\bar{\tilde{e}}_R$

[34] J. L. Feng *et al.*, *Phys. Rev.* **D52**, 1418 (1995).

https://doi.org/10.1017/9781009289801.016 Published online by Cambridge University Press

pair production, it is possible to test this relationship in experiments at the LC at the $\sim 1-2\%$ level, as illustrated in Fig. 15.22. If squarks are much heavier than sleptons, radiative corrections cause a significant splitting $\delta g' = g_{\tilde{B}\tilde{e}_R e}/\sqrt{2} - g'$ between these couplings: for instance, if squarks are an order of magnitude heavier than sleptons, this difference would be about 2%. A measurement of $\delta g'$ could thus provide an *upper bound* on the squark mass scale, even though the squark production threshold may be far beyond the available center of mass energy.[35]

A similar test of supersymmetry that may be possible if charginos are light instead is the subject of the following exercise. The message of this discussion is that LC experiments offer a unique opportunity for these *direct tests* of SUSY and, further, that these entail a study of just the lightest charged sparticles.

Exercise *Show that supersymmetry implies that the sum of squares of the off-diagonal entries in the MSSM chargino mass matrix is completely determined by M_W^2. This follows from the fact that the coupling of the Higgs scalar fields to the charged higgsino–charged gaugino system is determined by the gauge interaction. If charginos are light and have substantial mixing with higgsinos (as is the case, for instance, in the HB/FP region) it is possible to extract the required off-diagonal mixing elements from the chargino mass and production properties.*

If instead charginos are gaugino-like, a test analogous to our discussion in the text may be possible. The point is that it may be possible to extract the gaugino–sneutrino–electron coupling from chargino production data, allowing a test of the SUSY relationship between it and the $SU(2)$ gauge coupling.

Other measurements

Many other measurements are possible at linear colliders, but the details depend on which sparticle states are kinematically accessible, and also on the details of the SUSY model. For instance, if both $\widetilde{W}_1$ and $\widetilde{W}_2$ are kinematically accessible, and their masses as well as production cross sections with longitudinally polarized beams can be measured, a complete reconstruction of the chargino mass matrix would be possible.[36] On a different note, within the GMSB framework, the determination of the lifetime of a charged NLSP with a decay length as small as a millimeter may be possible in experiments at a LC, depending upon capabilities of the detector, though determinations of sparticle decay lengths exceeding ~ 50 m will be difficult.[37] The corresponding determination also appears possible for the case of a neutralino

[35] M. Nojiri, D. Pierce and Y. Yamada, *Phys. Rev.* **D57**, 1539 (1998); H-C. Cheng, J. Feng and N. Polonsky, *Phys. Rev.* **D57**, 152 (1998).
[36] S. Y. Choi *et al.*, *Eur. Phys. J.* **C14**, 535 (2000).
[37] P. Mercadante, J. K. Mizukoshi and H. Yamamoto, *Phys. Rev.* **D64**, 015005 (2001).

https://doi.org/10.1017/9781009289801.016 Published online by Cambridge University Press

NLSP, as long as its decay length is in a similar range.[38] We remind the reader that in these models the NLSP lifetime yields a measure of the fundamental SUSY breaking scale.

Finally, we note that in the initial phase of the LC only the lowest lying states will be accessible. Except for the LSP, these will be the easiest to detect and study in detail, since they are free of contamination from other SUSY reactions, have relatively simple decays, and the SM backgrounds to their signals will be well known. In contrast, at the LHC, or when much higher energies are attained at a LC, many SUSY reactions will be occurring simultaneously, and the heavy sparticle decays will be very complex. Knowledge of the lower lying states will prove very useful for disentangling the complicated cascade decay chains expected at the LHC as well as for a study of the more massive sparticles that may be accessible at an energy upgrade of a future LC. For this reason, it would be useful to archive the LHC data in a form suitable for reanalysis once data from a LC becomes available.

15.5.3 Models of sparticle masses: a bottom-up approach

Although the mechanism by which superpartners of SM particles obtain their masses is not known, we saw in Chapter 11 several models of sparticle masses have been proposed. These models differ from one another in that they rely on different assumptions about how the effects of SUSY breaking are communicated from the supersymmetry breaking sector to the MSSM sparticles. Although these models are simple in that sparticle masses and couplings are all determined by just a small set of parameters, it should be remembered that these models are all based on untested assumptions and may turn out to be wrong. Fortunately, if sparticles are discovered, and their properties determined at future colliders, it will be possible to subject these models to experimental tests, and perhaps even determine some of the underlying parameters.

The basic idea is very simple. Any model with a fixed number of adjustable parameters is tested if the number of independent observables exceeds the number of parameters. This is so because the values of parameters that reproduce some of the observables will not automatically also yield the observed values for all of them. In practice, of course, things are more complicated because both experimental measurements as well as theoretical predictions are subject to error, and, further, the sensitivity of observables to the different parameters is not the same. The usual approach for testing any particular framework is to perform a global fit to all relevant experimental data – in addition to sparticle masses, event rates and distributions (possibly, with polarized beams) for various signals, this includes

[38] S. Ambrosanio and G. Blair, *Eur. Phys. J.* **C12**, 287 (2000).

https://doi.org/10.1017/9781009289801.016 Published online by Cambridge University Press

low energy measurements such as branching fractions for rare decays, anomalous electric and magnetic moments of leptons or the neutron, as well as cosmological data such as the determination of cold dark matter relic density – and perform statistical tests for the goodness of fit. If a good fit is obtained (some of) the underlying parameters can be extracted; otherwise, a particular framework is excluded.

We have already seen the start of such a program in our discussion of the "allowed" and "excluded" regions of the parameter space of the mSUGRA model. It is straightforward to carry out similar studies for other scenarios. Of course, once direct information about sparticle properties becomes available, such studies will rapidly exclude many scenarios, perhaps even all the simple ones that we discussed in Chapter 11. In this case, we hope that these data will suggest how to proceed, and allow us to synthesize the mechanism by which superpartners acquire their masses.

Several groups have also examined how well experiments at the LHC or the LC will be able to extract the underlying model parameters. These studies have typically been carried out within the mSUGRA as well as GMSB frameworks. What is done is to use Monte Carlo methods to construct a synthetic data sample (within say the mSUGRA model) which is then "analyzed" to see how well the underlying parameters can be reconstructed from the various observables. It is not our purpose to discuss this in detail, and we will refer the reader to the studies in Technical Design Reports (TDRs) of ATLAS and TESLA, as well as to other studies in the literature.

Not surprisingly, the precision with which the underlying parameters can be extracted is sensitive to where one is in parameter space. For the mSUGRA model, m_0 and $m_{1/2}$ set the scale of squark and gluino/gaugino masses and can, in favorable cases, be extracted to better than 5–10% at the LHC, though the errors are somewhat larger if $\tan\beta$ is large. In fortuitous circumstances where isolation of a particular decay chain allows $m_{\widetilde{Z}_2} - m_{\widetilde{Z}_1}$ to be very precisely determined from a dilepton mass edge, $m_{1/2}$ can be determined to within a percent. A more precise determination of m_0 may be possible if the mass edges from $\widetilde{Z}_2 \to \tilde{\ell}_R \ell \to \ell\ell\widetilde{Z}_1$ can be constructed. Determination of $\tan\beta$ and A_0 is more difficult.[39]

If sleptons (charginos) are accessible at a LC, the determination of their masses will yield m_0 and $m_{1/2}$ at the percent level or better depending on the integrated luminosity. The TESLA TDR quotes a precision better than a part per mille on this. Also, for the case study in the TESLA TDR where both $\tilde{\tau}_1$ and $\tilde{\tau}_2$ are kinematically accessible, it is claimed that $\tan\beta = 3 \pm 0.02$, and $A_0 = 0 \pm 6$ GeV. While the sensitivity to these parameters will depend on the precision with which third generation masses are ultimately determined (see our comments in Section 15.5.2),

[39] In several of the ATLAS studies, it appears that $\tan\beta$ is determined. Notice, however, that this is because m_h in these studies is relatively light (below the bounds from LEP2); m_h becomes increasingly less sensitive to $\tan\beta$ if it is close to its theoretical upper limit.

https://doi.org/10.1017/9781009289801.016 Published online by Cambridge University Press

experiments at LCs will certainly provide new information. If sleptons are accessible, their masses will pin down m_0 more precisely than experiments at the LHC, and if stau or stop mixing angles can be determined we will obtain information about the other parameters.

At the LHC, the optimal strategy for the extraction of MSSM masses and other weak scale parameters depends sensitively on the model, as well as where we are in parameter space, so that it is not possible to map out how to proceed ahead of time. However, we may say with some confidence that, with some guidance from the data, it will likely be clear how to proceed, and that it is also likely that we will glean more information than is currently thought possible. Experiments at a LC, in contrast, allow a beautiful and systematic program for these measurements that will truly complement the capabilities of the LHC. Here, we have only been able to touch upon some of the exciting capabilities of these machines. Exploration of what might be possible at both these facilities has only just begun, and is an active and fruitful area of research.

15.6 Photon, muon, and very large hadron colliders

Some possibilities for other future colliders include photon–photon and electron–photon colliders operating at a center of mass energy just below that of an available electron–positron collider, muon colliders operating in the TeV region, and also a very large hadron collider (VLHC) which might operate at $\sqrt{s} = 40$–200 TeV to succeed the LHC.

High energy photons can be produced by back scattering laser photons from a high energy electron beam. The maximum photon energy is typically about 80% of the electron beam energy. Moreover, the scattered photons are (partially) polarized if the initial electron and the laser photons are polarized. Since an electron Compton back scatters multiple times as it passes through the laser pulse, a high energy e^-e^- collider can be converted to a $\gamma\gamma$ collider with comparable luminosity, but with a distribution of collision energies and photon polarizations. While there is no particular advantage of this as far as sparticle searches go, the availability of polarized photon beams is especially useful for a study of MSSM Higgs bosons. First, the rate for single Higgs boson production depends on all charged sparticle states that dominantly acquire their mass via a coupling to the Higgs, so that from this rate we can "count" all these new states. For supersymmetry aficionados, it is more interesting that the amplitude for the production of CP-odd and CP-even Higgs scalars by photon–photon collisions depends differently on the polarizations of the initial photons.[40] If CP is not conserved, a study of any Higgs boson resonance for

[40] This should not be surprising, since parity arguments would tell us that the leading order matrix element must be proportional to $\boldsymbol{\epsilon_1} \cdot \boldsymbol{\epsilon_2}$ ($\boldsymbol{\epsilon_1} \times \boldsymbol{\epsilon_2} \cdot \hat{\mathbf{p}}_{\rm Higgs}$) if the CP of the Higgs boson is even (odd), where $\boldsymbol{\epsilon_1}$ and $\boldsymbol{\epsilon_2}$ are the polarization vectors of the two photons.

https://doi.org/10.1017/9781009289801.016 Published online by Cambridge University Press

different photon polarizations would yield information about its CP content. It may also be possible to run the collider in the $e\gamma$ mode, in which case processes such as $e\gamma \to \tilde{e}_{L(R)}\widetilde{Z}_1$ may allow us to access selectrons beyond the kinematic reach of an electron–positron collider with corresponding energy.

A muon beam has the advantage of low energy losses due to synchrotron radiation, so that a circular collider operating in the TeV region and with a much more precisely tuned beam energy relative to an electron–positron collider can be envisioned. The challenge, of course, is that the muons in the beam are unstable, so that storage, acceleration, and collisions must occur before these decay away. In addition, there are significant background problems from decays of muons in the beams. The large muon Yukawa coupling relative to that of the electron provides a unique capability: at a muon collider it is possible to produce neutral Higgs bosons in the s-channel at a large rate, allowing for detailed Higgs boson studies in much the same way that LEP has studied the Z boson. This is especially true for the more massive states such as H and A in the MSSM. Otherwise, capabilities for SUSY particle production are qualitatively similar to those of an e^+e^- collider operating in the same energy regime, except that at a muon collider, smuon pair production would occur at large rates due to t-channel graphs, whereas selectron pair production would only occur via s-channel graphs.

A very large hadron collider (VLHC) is a broad band machine that would search for new physics up to the 10–20 TeV scale, depending on the center of mass energy. While it is reasonable to see what LHC data tell us about new physics, it is worth mentioning that there can be many scenarios where the VLHC may prove essential. These include, for instance, models with additional Z bosons or with (multi-TeV scale) extra spatial dimensions. In the case of weak scale supersymmetry, a VLHC would be useful in the event that SUSY particle masses are in the TeV or multi-TeV region. In the case of GMSB models, it might also be possible at a VLHC to search for the messenger states, along with the superpartners. We note that TeV scale sparticle masses may be realized in the HB/FP region of the mSUGRA model, or in inverted hierarchy models, where just first and second generation squarks and sleptons are in the multi-TeV region. To date, few detailed studies exist for such very high energy hadron colliders.

https://doi.org/10.1017/9781009289801.016 Published online by Cambridge University Press